Austrian Journal of Earth Sciences | Vienna | 2016 | Volume 109/1 | 29 - 44 | DOI: 10.17738/ajes.2016.0002

Aquifer geochemistry of crystalline rocks and Quaternary deposits in a high altitude alpine environment (Kauner Valley, Austria)

Thomas STRAUHAL[1) 2)*)], Christoph PRAGER[1) 3)], Bernard MILLEN[4)], Christoph SPÖTL[2)], Christian ZANGERL[1) 5)] & Rainer BRANDNER[2)]

[1)] alpS – Centre for Climate Change Adaptation, Grabenweg 68, 6020 Innsbruck, Austria;

[2)] Institute of Geology, University of Innsbruck, Innrain 52f, 6020 Innsbruck, Austria;

[3)] ILF Consulting Engineers Austria GmbH, Feldkreuzstraße 3, 6063 Rum, Austria;

[4)] GEOCONSULT Consulting Engineers, Hölzlstraße 5, 5071 Wals, Austria;

[5)] Institute of Applied Geology, University of Natural Resources and Life Sciences, Peter-Jordan-Straße 70, 1190 Vienna, Austria;

[*)] Corresponding author, strauhal@alps-gmbh.com

KEYWORDS hydrochemistry; water-rock interaction; isotopes; spring water; tunnel water inflow; Austria

Abstract

In the Upper Kauner Valley of the Tyrolean Central Alps in Austria, some of the slopes, consisting of crystalline bedrock covered by Quaternary deposits, host groundwater of remarkable chemical composition. The bedrock consists mainly of a thick paragneiss series with intercalations of orthogneiss and amphibolite belonging to the Ötztal-Stubai Basement Complex. These metamorphic rocks are ubiquitously fractured and the fracture surfaces are coated with Fe-(hydr-)oxides and chlorite but also carbonates. Sulphides occur as dispersed accessory crystals and locally as small ore deposits. During the Quaternary, the valley floor, slopes, and cirques were covered by clastic sediments of differing thicknesses. A striking feature of the valley is that the slopes have been affected by different types of mass movements (rockfalls, debris flows and deep-seated rockslides). Data from extensive (hydro)geological field surveys, tunnels (exploration drift and water conduction galleries) and exploration drillings indicate that the groundwater preferentially flows within zones of highly weathered bedrock (i.e. the saprolite), brittle fault and fracture zones, deep-seated rockslides, and in the conductive Quaternary deposits, i.e. the talus, colluvium, debris flow and alluvial deposits. Interestingly, unusually high amounts of total dissolved solids (>1000 mg/l) were measured in some spring waters. Tritium and $\delta^{18}O$ values indicate short residence times (<5 years) and the analysis of $\delta^{18}O$ and $\delta^{2}H$ data shows that the groundwater is of meteoric origin and that no fractionation or evaporation processes, leading to increased mineralisation, have taken place. Ca and Mg are the dominant cations and SO_4 and HCO_3 are the major anions present. Data correlation shows that the electric conductivity (EC) of the waters increases with increasing Ca, Mg and SO_4 concentration, but not with HCO_3. Low $\delta^{34}S$ values indicate that the dissolved sulphate can be attributed to the oxidation of sulphides. Accordingly, the dissolution of carbonate fracture fillings and the oxidation of pyrite and other sulphides are regarded as the main processes responsible for the mineralised groundwater in the study area.

Im hinteren Kaunertal der Tiroler Zentralalpen, welches aus metamorphen Gesteinen aufgebaut und durch quartäre Ablagerungen bedeckt wird, tritt Grundwasser von bemerkenswerter chemischer Zusammensetzung auf. Das Festgestein ist Teil des Ötztal-Stubai-Komplexes und besteht vorwiegend aus mächtigen Paragneis-Serien mit Einschaltungen aus Orthogneis und Amphibolit. Diese metamorphen Gesteine treten durchgehend geklüftet auf. Die Kluftflächen weisen Fe-(hydr-)oxide und Chlorit sowie Karbonatüberzüge auf. Sulfide treten einerseits feinverteilt akzessorisch und andererseits als kleine Erzkörper auf. Im Quartär wurden klastische Sedimente unterschiedlicher Mächtigkeiten im Talboden, auf den Hängen und in hochgelegenen Karen abgelagert. Ein besonderes Merkmal des Tales sind verschiedene Typen von Massenbewegungen (Steinschlag, Muren und tiefgründige Felsgleitungen), die entlang der Hangflanken auftreten. Daten von umfassenden (hydro)geologischen Gelände- und Tunnelaufnahmen (Erkundungsstollen und Wasserbeileitungsstollen) zeigen, dass das Grundwasser vorwiegend in stark verwitterten Bereichen des Festgesteins (Saprolit), in spröden Störungs- und Zerlegungszonen, in tiefgründigen Massenbewegungen und den durchlässigen quartären Ablagerungen, wie alluvialen Sedimenten, Murschutt, Hangschutt und kolluvialen Schuttkegeln, fließt. Interessanterweise wurden ungewöhnlich hohe Gesamtionenkonzentrationen (>1000 mg/l) in einigen der natürlichen Quellwässer gemessen. Die Tritium und $\delta^{18}O$ Gehalte deuten auf kurze Verweilzeiten (<5 Jahre) hin. $\delta^{18}O$ und $\delta^{2}H$ Daten zeigen, dass das Grundwasser meteorischen Ursprungs ist und keine Fraktionierung oder Evaporation stattgefunden haben, welche die Mineralisation erhöhen würden. Ca und Mg sind die dominierenden Kationen, und SO_4 und HCO_3 treten als Hauptanionen auf. Eine Korrelation der Daten zeigt, dass die elektrische Leitfähigkeit des Wassers mit zunehmenden Ca, Mg und SO_4 Werten, jedoch nicht mit zunehmender HCO_3 Konzentration steigt. Niedrige $\delta^{34}S$ Werte weisen darauf hin, dass das gelöste Sulfat aus der Oxidation von Sulfiden stammt. Die Lösung von karbonatischen Kluftfüllungen und die Oxidation von Pyrit und anderen Sulfiden werden somit als Hauptprozesse für die hohe Mineralisation des Grundwassers im Untersuchungsgebiet angesehen.

1. Introduction

Low amounts of total dissolved solids are typically characteristic for young groundwater from silicate rock aquifers (e.g. phyllite, schist, gneiss; Reichl et al., 2001; Kilchmann et al., 2004; Krásny and Sharp, 2007; Singhal and Gupta, 2010), reflecting the low solubility of the rock-forming minerals (Tóth, 1999; Hölting and Coldewey, 2013). Only intensive water-rock interactions occurring during long residence times and/or high aquifer temperatures lead to increased concentrations of dissolved silica and other elements (e.g. Na and K) in such aquifers (e.g. Bucher et al., 2009; Hölting and Coldewey, 2013). On the other hand, non-silicate minerals, in particular carbonates, sulphides and sulphates, which occur as accessory minerals disseminated in the rock and/or as fracture coatings and fillings, often have a larger impact on groundwater chemistry than the main rock-forming silicate minerals due to their higher reactivity (e.g. White et al., 1999; Kilchmann et al., 2004; Frengstad and Banks, 2007; Hölting and Coldewey, 2013). Given that accessory minerals and fracture coatings generally only occur in low quantities (White et al., 1999, 2005), and that the reactive surfaces in most crystalline rock aquifers are restricted to the hydraulically active fractures, the amount of total dissolved solids in the groundwater in the majority of shallow crystalline rock aquifers is low. According to the hydrochemical study of Kilchmann et al. (2004) in the Swiss and French Alps, groundwater from crystalline rocks is generally of the Ca-HCO_3-SO_4 type and dilute (22 to 158 mg/l total dissolved solids). Similarly, the groundwater from silicate rock aquifers in Tyrol, which includes the study area, is mainly of the Ca-HCO_3 type (Kralik et al., 2005). Bucher et al. (2012) presented a wide variety of water compositions and water-mineral interactions from deep water samples from the Gotthard rail base tunnel. They conclude that water in the crystalline basement receives the dissolved solids from dissolution of albite and secondary calcite, Fe-sulphide oxidation, alteration of biotite to chlorite and from leaching of soluble inclusions in pores and minerals.

In contrast to Kilchmann et al. (2004) and Kralik et al. (2005), the chemical composition of some of the groundwater presented herein has high amounts of total dissolved solids unusual for young waters emerging from crystalline rocks and in Quaternary deposits.

The aim of this study was to identify the processes giving rise to this groundwater chemistry and the possible influence of mass movements. The conclusions presented herein are the result of extensive hydrochemical and isotopic analyses of the groundwater and geological, mineralogical and geotechnical surveys.

2. Study area

The study area lies within the Upper Kauner Valley, Tyrol, Austria (Figure 1). This north-south trending valley is surrounded partly by glaciated mountains with summits up to about 3500 m asl. During glacial maxima, the valley was filled by a glacier with an ice surface reaching up to 2800 m asl (van Husen, 1987) resulting in a glacially sculptured U-shaped morphology.

The (hydro)geological investigation area extends from the valley floor (approximately 1600-1800 m asl) up to the summit ridges at around 3500 m asl and comprises the valley slopes, tributary valleys and gullies and large cirques at higher altitudes (Figures 1 and 2).

Since 1964, the valley floor has been filled by the Gepatsch Reservoir (maximum water surface level 1767 m asl; TIWAG-Tiroler Wasserkraft AG). The dam at the northern end of the reservoir reaches 153 m in height. Water is diverted into the reservoir, from other catchment areas, by two conduction galleries (Radurschl and Pitztal), whereby the rock mass overburden above these galleries reaches approximately 1000 m in the study area. The reservoir also receives natural water inflow from the Fagge Stream flowing from the south.

Extensive (hydro)geological field surveys, exploration drilling campaigns, geodetic monitoring and exploration drifts (tunnels) carried out since the 1960's by the hydropower company TIWAG-Tiroler Wasserkraft AG show that the reservoir slopes, particularly those consisting of paragneiss, have been affected by several deep-seated, slowly creeping rockslides. These detailed site investigations examined the interaction between the mass movements and the operation of the Gepatsch Reservoir (e.g. Lauffer et al., 1967; Lauffer, 1968; Tentschert, 1998; Zangerl et al., 2010; Schneider-Muntau, 2012 and unpublished internal TIWAG-Tiroler Wasserkraft AG reports). The recent site investigations comprised several drillings and the construction of the 690 m-long Klasgarten Exploration Drift (Holzmann and Hofer, 2012), which provided fundamental insights into the geotechnical and hydrogeological characteristics of both the bedrock and the mass movements. In the Klasgarten Exploration Drift the overburden reaches up to 170 m and is characterised by the strongly fragmented rocks of the deep-seated Klasgarten Rockslide over long stretches (Figure 1).

3. Geological setting

3.1 Bedrock

A several hundred metre-thick paragneiss series with intercalations of orthogneiss and amphibolite (Hammer, 1923 a, b; Purtscheller, 1978) belonging to the south-western part of the Ötztal-Stubai Basement Complex of the Eastern Alps (Schmid et al., 2004) constitutes the bedrock of the study area.

The dominant components of the paragneiss are quartz, mica (mainly biotite), chlorite, plagioclase and orthoclase (Hammer, 1923 a). Typical characteristics of the paragneiss at the surface (and down to a few metres depth) and in the rockslides are the reddish-brown coloured fracture and block surfaces indicating substantial (sub)surface weathering. The fractures show a close to moderate spacing (6 to 60 cm) and the rock block shapes are mainly tabular.

The orthogneiss is composed mainly of quartz, plagioclase, orthoclase and mica (largely muscovite; biotite is partly chloritised). The fractures within the orthogneiss are mode-

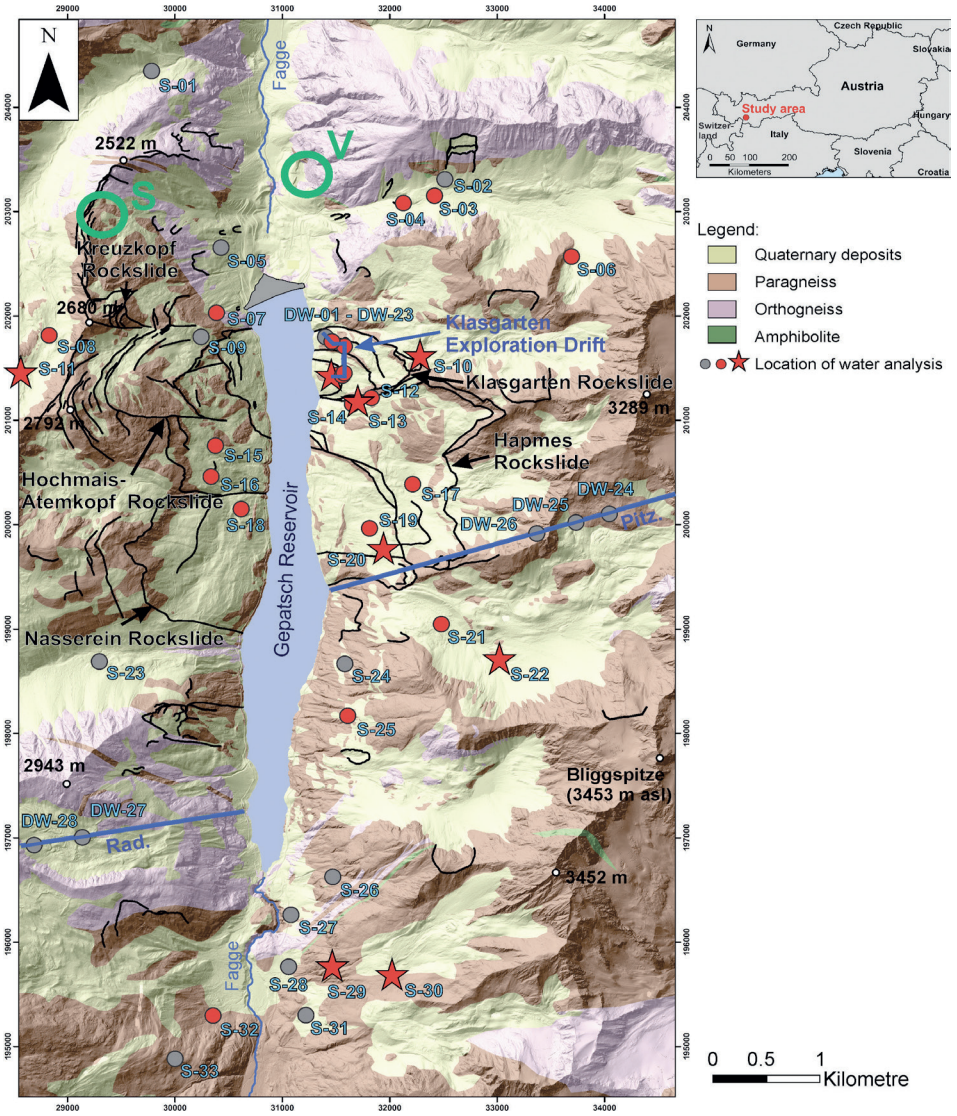

Figure 1: Locations of the studied springs (S-**) and tunnel (drift and galleries) water inflows (DW-**). The sample locations are symbol- and colour-coded according to the water chemistry (Figure 6): Samples with a (Ca+Mg)/SO_4 ratio of 1 (±10 %) are highlighted red; samples with a Ca:Mg:SO_4 ratio of 2:1:3 (±10 %) are highlighted with a red star; main lithological units are according to Zangerl et al. (unpublished map and report, 2013) and Hammer (1923 b); scarps of landslides illustrated in black; green circles illustrate the locations of the ore deposits S…"Sudleskopf" and V…"Versetz" in the northwest and in the north, respectively; Rad. … Radurschl Water Conduction Gallery, Pitz. …Pitztal Water Conduction Gallery; maximum Gepatsch reservoir level: 1767 m asl.

rately to widely spaced (20 to 200 cm) forming mainly blocky rock mass shapes.

Banded amphibolites occur locally as thin intercalations, mainly in association with the orthogneiss (Hammer, 1923 a, b; Purtscheller, 1978). The main components of the amphibolites are plagioclase, hornblende and quartz.

In general, the observed abundance of fractures in the orthogneiss is lower than in the paragneiss series. Due to this and an intense foliation, the weaker paragneiss is more prone to form deep-seated, creeping rockslides (Tentschert, 1998; Zangerl et al., 2010; Schneider-Muntau, 2012; Holzmann and Hofer, 2012; Zangerl et al., unpubl. report 2013).

The extensive (hydro)geological subsurface investigations (drillings, drifts) have revealed that the paragneiss and orthogneiss bedrock in the study area is characterised by a similar range of hydraulic conductivities typically between about 10^{-7} and 10^{-9} m/s with the local fracture zones reaching values of up to about 10^{-5} m/s (results of hydraulic packer tests; unpublished data TIWAG-Tiroler Wasserkraft AG).

3.2 Ore deposits

Small metamorphosed ore deposits occur at two locations in the study area (Figure 1) associated with Pre-Variscan (meta)magmatites (Weber, 1997; Vavtar, 1997). The first site is located close to Sudleskopf in the northwest of the study area, and contains galena (PbS), pyrite (FeS_2) and chalcopyrite (Cu-FeS_2), ± arsenopyrite (FeAsS), ± magnetic pyrite (FeS-Fe_5S_6,), ± sphalerite (ZnS), ± boulangerite ($Pb_5Sb_4S_{11}$), ± fahlore (Cu, Fe, Zn, Ag, Hg)$_{12}$[S/As_4S_{12}] – (Cu, Fe, Zn, Ag, Hg)$_{12}$[S/Sb_4S_{12}]), ± bournonite ($PbCuSbS_3$), ± marcasite or pyrite (FeS_2) and ± covellite (CuS). The sulphur isotopic composition suggests a magmatic origin of these ore minerals ($\delta^{34}S \approx 0$ ‰ – Vienna Cañon Diablo Troilite; Vavtar, 1979). Galena shows high concentrations of Ag, Cu, Fe and Sb. Associated minerals are quartz, ferrous dolomite to ankerite, and minor calcite (Vavtar, 1988).

The second ore deposit, Versetz, at the northern boundary of the study area is characterised by 10-20 cm-thick deposits consisting of galena, magnetic pyrite, chalcopyrite and calcite (Matthias, 1961 in Vavtar, 1988).

Thin section analyses obtained from the drill cores in this study area show that small amounts of dispersed ore minerals are also commonly present as accessory minerals in paragneiss (Figure 3 a).

3.3 Fracture minerals

Several types of secondary minerals occur as fracture fillings or coatings within the bedrock, the rockslides and Quaternary deposits. Especially in the paragneiss, greenish-black chloritic coatings, reddish-brown weathering minerals such as limonite and Fe-(hydr-)oxides and altered biotites are

abundant (Figure 3 b-d). The Fe-rich coatings most likely originated from the oxidation of pyrite and other sulphide minerals. Areas affected by brittle tectonic and/or mass movements show a higher degree of weathering than intact bedrock.

Calcitic and dolomitic fracture coatings are mainly associated with chlorite and dominantly occur within tectonically formed shear and fracture zones. Furthermore along the shear zones, large crystals (cm range) of muscovite and kyanite are present. In the Verpeil Valley (about 4 km north of the investigation area) Bernhard (2008) reported a variety of minerals, e.g. gypsum, andalusite, stilbite and native sulphur. Prehnite and zeolithe were also found in this area as fracture fillings in the orthogneiss.

3.4 Quaternary deposits

Till covers large expanses of the study area. These glacial sediments consist of a clay- and silt-rich matrix and clasts of paragneiss, quartzite, orthogneiss and amphibolite. These deposits generally reach a few metres but locally up to several tens of metres in thickness.

Several types of mass movements are located in the study area: a) deep-seated rockslides (Figures 1 and 2), b) rockfalls which form talus deposits, and c) debris flows in steep gullies forming colluvial cones. Deformation during gravitational movement of the rockslides produced intense and large fragmentation of the bedrock down to depths of more than 100 m. At the bottom of the Kauner Valley, the exploration drillings revealed that the alluvial deposits consist of varying amounts of gravel, sand, and silt with thicknesses of several tens of metres. Minor alluvial deposits are located also at the bottom of some tributary valleys.

At altitudes above about 2100 m asl, several active, inactive and fossil rock glaciers are present (Piccolruaz, 2004; Krainer et al., 2007; Krainer and Ribis, 2012). Most of them are located in the high altitude tributary valleys and cirques.

4. Methods

Extensive (hydro)geological field mapping (~45 km^2, Figure 1), drillings and tunnel surveys have been performed. About 500 springs were mapped during hydrogeological field surveys in 2009 and 2010 (Figure 2). Water temperature (°C) and electric conductivity (EC; µS/cm) were measured using portable instruments. Thirty three of these springs (S-01 to S-33) were then selected for hydrochemical analyses to investigate the water-rock interactions in the recharge areas and the groundwater flow systems (Figures 1 and 11). Twenty one springs were analysed at intervals of three months (chemistry) and one month (stable isotopes), respectively, for a period of up to 19 months. The groundwater chemistry was also analysed at 23 different inflows (DW-01 to DW-23) into the Klasgarten Exploration Drift (Figure 1). These data were compared with analyses obtained from groundwater inflows at five locations into two existing water conduction galleries, 'Pitztal' (DW-24, DW-25 and DW-26) and 'Radurschl' (DW-27 and DW-28, Figure 1) sampled in 2011 by GEOCONSULT Consulting Engineers and analysed by Wasser Tirol – Wasserdienstleistungs-GmbH.

Water sampling was performed according to the Austrian and European standard ÖNORM EN ISO 5667-3 (2013) using 500 ml polyethylene bottles. The pH values and major ion concentrations (Ca, Mg, Na, K, HCO_3, Cl, NO_3, NO_2, o-PO_4, SO_4, F and in some cases NH_4, Fe, Mn, Sb, As, Al, Pb, Cd, Cr, Cu, Ni and Zn), as well as $\delta^{18}O$, $\delta^{2}H$ (reported in ‰ VSMOW – Vienna Standard Mean Ocean Water), ^{3}H (given in Tritium Units, TU) and $\delta^{34}S$ (in ‰ VCDT) were determined by titration, photometry, inductively coupled plasma optical emission spectrometry (ICP-OES), ion-chromatography (IC) by Wasser Tirol – Wasserdienstleistungs-GmbH (ions) and mass spectrometry by Hydroisotop GmbH (isotopes), respectively, according to the national standards ÖNORM EN 9963-1 (1996), ÖNORM EN ISO 11885 (2009), EPA 350.1 (1993), DIN 38406 E5 (1983), DEV (1994), ÖNORM EN ISO 10304-1 (2012) and ÖNORM EN 26777 (1993).

Rockware AqQA Version 1.1.1 (RockWare Inc., 2006) was used to evaluate the hydrochemical data and calculate charge balance errors (cf. Table 1). Almost all the water analyses passed the test for internal consistency.

Saturation indices (SI) of calcite, aragonite, dolomite,

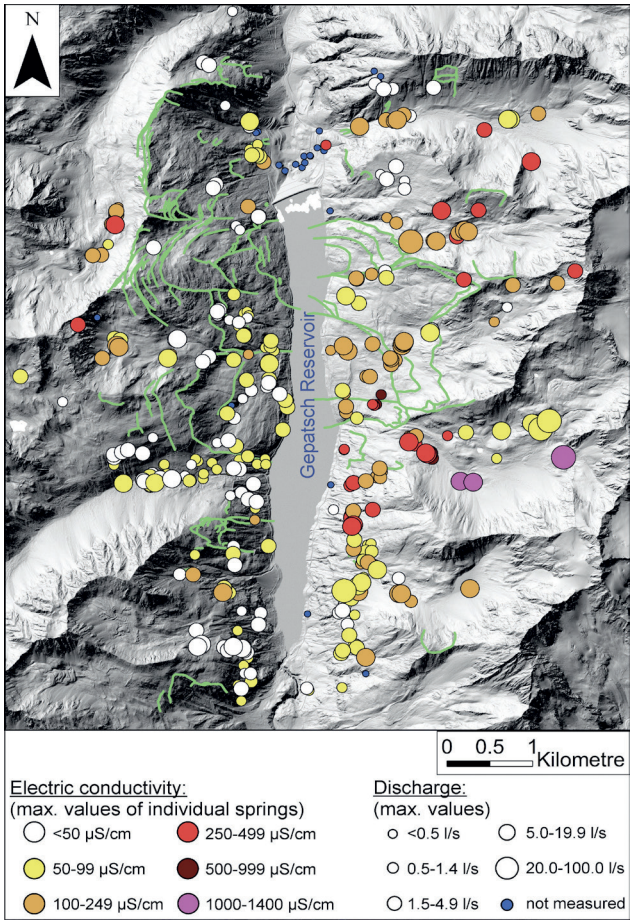

Figure 2: Spatial distribution and depiction of the electric conductivity and discharge of the mapped springs as encountered during field surveys (n = approximately 500). Scarps of landslides are shown in green.

Figure 3: a) Opaque, fine grained ore minerals (predominantly pyrite) in a thin section of paragneiss from a drill core obtained from the orographic right valley slope (parallel nicols; image source: Wasser Tirol); b) orthogneiss and c) paragneiss samples showing centimetre- to decimetre-wide calcite (white) and chlorite (black) fracture fillings; d) reddish-brown altered paragneiss with calcitic fracture filling.

Anion sum [meq/l]	Acceptable difference
0 – 3	± 0.2 meq/l
3 – 10	± 2 %
10 – 800	± 5 %

Table 1: Rules for the internal consistency of the water samples on the basis of the cation/anion ratios (according to Rockware Inc., 2006).

anhydrite, gypsum, haematite and goethite were calculated using PHREEQC Interactive 3.1.1 (Parkhurst and Appelo, 1999). A default pe-value (e.g. Merkel and Planer-Friedrich 2008) of 4 was used for all calculations.

Thin sections were analysed and X-ray powder diffraction analyses were done at the Institute of Mineralogy and Petrography, University of Innsbruck, to determine the mineralogical composition of the bedrock and fracture coatings. X-ray fluorescence spectroscopy was used to examine the elemental composition of bedrock samples (Strauhal, 2009).

5. Results

5.1 Groundwater chemistry

The EC of all mapped springs (n = approximately 500) ranges widely between 15 and 1400 µS/cm (Figure 2). Springs situated on the orographic right side of the valley have noticeably higher EC values than those on the left side. The highest values were measured at springs emerging at the mouths of high altitude tributary valleys (Figure 2).

The spring waters are predominantly neutral to slightly alkaline (pH 7.1 to 7.9). Only a few have slightly acidic values (e.g. S-08: pH 5.0). These lower pH-values were measured at springs which are located close to Sudleskopf ore deposits (abandoned mine).

The EC of groundwater inflows in the Klasgarten Exploration Drift ranges from approximately 70 to 740 µS/cm. Sections of the drift, which are located in the Klasgarten Rockslide, have slightly higher EC values (dominantly 230-340 µS/cm) than sections in the surrounding in-situ bedrock (dominantly 180-230 µS/cm). In the drift, some of the water inflows are characterised by very high pH-values of up to 11.6. Such values are related to the tunnel drive (groundwater interaction with fresh shotcrete which is used as an immediate tunnel support system).

The dominant cations and anions present in the spring waters are Ca and Mg, and SO_4 and HCO_3, respectively (Figure 4 and Table 2) and the majority of the spring waters can be classified as a Ca-Mg-SO_4 type (major cations and anions in descending order where normalised equivalent concentrations are ≥ 20 % – Table 2). Sulphate is by far the most abundant anion present, especially in the water emerging from the orographic right valley slopes. Cl, NO_3 and Mn are below the limit of detection in all spring waters except for S-08 which is rich in Mn (approximately 160 µg/l). F is present in many spring waters at concentrations <1.2 mg/l. Na, K, NO_2, PO_4 and Fe were below or close to the detection limit in most samples. However, there are spring waters present where Na is a dominant cation, but these springs (S-09, S-15, S-16 and S-27) generally have low EC values (Table 2). The highest concentrations of Ca+Mg and SO_4 (270 and 766 mg/l, respectively; S-22) were measured on the orographic right side of the valley. Remarkably high As concentrations of up to 20 µg/l were analysed at S-23 at the western end of the study area (Figure 1).

The hydrochemistry of the water inflows in the Klasgarten Exploration Drift are similar to the nearby springs emerging naturally at the surface (Tables 2 and 3). Some of the tunnel water inflows are characterised by higher Na, F and Cl and lower Ca concentrations than the springs. However, the only clear differences between springs and tunnel water inflows

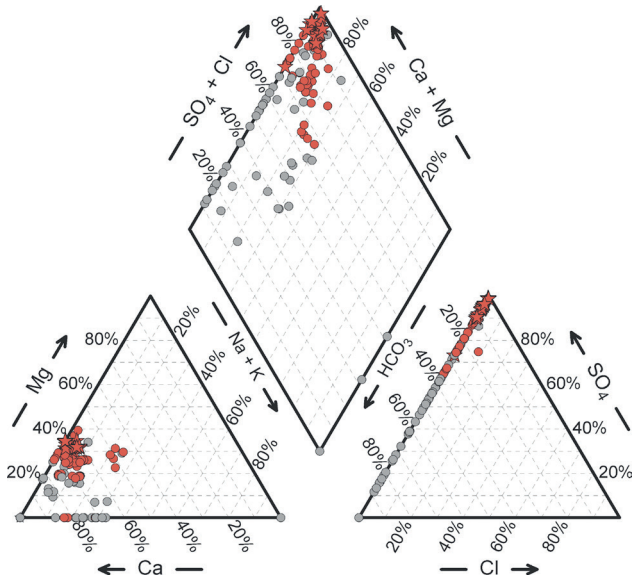

Figure 4: Major ion chemistry of the analysed water samples plotted in a Piper diagram to illustrate different water types as described in the text. The samples are symbol-coded according to the water chemistry (see captions of Figure 6).

Sample	X-Coord.	Y-Coord.	Altitude [m.asl]	Water-Type	EC [µS/cm]	T [°C]	pH	^{2}H [‰]	^{18}O [‰]	^{3}H [TU]	Ca [mg/l]	Mg [mg/l]	Na [mg/l]	K [mg/l]	HCO_3 [mg/l]	Cl [mg/l]	NO_3 [mg/l]	NO_2 [mg/l]	$o\text{-}PO_4$ [mg/l]	SO_4 [mg/l]	F [mg/l]	NH_4 [mg/l]	Fe [mg/l]	Mn [µg/l]	Sb [µg/l]	As [µg/l]
S-01	29773	204350	2003	Ca-Mg-SO_4-HCO_3	60	4.2	7.9	-99.2	-13.8	8.1	6.6	1.3	<1.5	[1.5]	10.4	[2.0]	[1.1]	[0.0]	[0.0]	18.1	0.2	0.0	<0.0	[0.0]	[0.7]	<1
S-02	32500	203321	2270	Ca-HCO_3	30	3.1	7.4	-106.3	-14.5	8.3	3.9	[0.9]	<1.5	[1.5]	12.2	[2.0]	<1.6	0.0	[0.0]	1.3	1.1	0.1	<0.0	<0.0	[0.7]	7.8
S-03	32402	203164	2209	Ca-Mg-SO_4	116	3.8	6.3	-109.8	-15.0	8.9	13.8	3.5	<1.8	[1.0]	10.4	[2.0]	[1.3]	[0.0]	[0.1]	42.6	0.2	[0.0]	[0.0]	0.6	[0.4]	[0.7]
S-04	32113	203093	2123	Ca-Mg-SO_4	240	2.9	6.7	-104.9	-14.5	8.2	29.6	6.9	2.1	<2.2	7.9	[2.0]	[1.1]	[0.0]	0.1	95.9	0.2	<0.0	<0.0	<0.0	[0.7]	<1
S-05	30417	202665	1817	Ca-HCO_3-SO_4	63	4.1	7.5	-103.6	-14.3	8.6	9.1	[0.9]	1.6	[1.5]	23.2	[2.0]	[1.1]	[0.0]	[0.0]	11.1	1.1	0.1	<0.0	<0.0	[0.7]	<1
S-06	33681	202585	2600	Ca-Mg-SO_4	408	1.0	7.4	-95.5	-13.4	n.m.	44.7	16.5	2.0	[1.5]	11.0	[2.0]	<1.6	<0.0	0.1	172.0	0.1	0.0	<0.0	0.0	[0.6]	[0.1]
S-07	30373	202048	1971	Ca-Mg-SO_4	136	2.0	7.3	-102.0	-14.1	8.4	14.2	3.7	3.0	[1.5]	6.7	[2.0]	<1.6	<0.0	[0.0]	49.1	0.1	0.0	<0.0	<0.0	[0.7]	[0.3]
S-08	28817	201826	2481	Ca-Mg-SO_4	294	0.9	5.0	-98.9	-13.7	9.8	29.9	12.3	1.5	<2	1.8	[2.1]	[1.6]	<0.0	[0.3]	131.7	0.3	0.1	<0.0	162.0	<1	n.m.
S-09	30229	201815	2125	Na-HCO_3-SO_4	15	3.8	8.0	-102.2	-14.1	7.7	<1.6	[0.9]	1.8	[1.5]	8.5	[2.0]	[1.1]	[0.0]	<0.1	3.2	0.2	0.1	<0.0	<0.0	[0.7]	[0.3]
S-10	32273	201620	2343	Ca-Mg-SO_4	142	2.2	6.3	n.m.	n.m.	n.m.	28.1	9.7	1.4	1.5	7.3	<1	1.5	n.m.	n.m.	107.0	<0.1	n.m.	n.m.	n.m.	n.m.	n.m.
S-11	28531	201454	2515	Ca-Mg-SO_4	147	3.3	6.2	-101.7	-14.1	9.4	15.7	4.8	<1	<2	6.1	[2.1]	[1.6]	<0.0	n.m.	60.1	[0.1]	0.1	<0.0	<20	<1	n.m.
S-12	31816	201228	2102	Ca-Mg-SO_4	142	4.3	6.4	n.m.	n.m.	n.m.	29.2	6.2	2.4	1.7	11.6	<1	<1	n.m.	n.m.	95.7	<0.1	n.m.	n.m.	n.m.	n.m.	n.m.
S-13	31672	201177	1987	Ca-Mg-SO_4	277	4.1	8.3	n.m.	n.m.	n.m.	27.7	6.1	2.4	<2	17.0	[1.6]	[1.5]	<0.0	<0.0	90.5	<0.2	[0.0]	<0.0	<0.0	<1	<1
S-14	31642	201171	1965	Ca-Mg-SO_4	214	4.5	n.m.	-102.0	-14.0	7.1	26.1	5.9	2.6	<2.2	12.2	[2.0]	[1.1]	0.0	<0.1	84.7	0.1	[0.0]	<0.0	<0.0	[0.7]	[0.3]
S-15	30361	200775	2072	Ca-Mg-Na-SO_4-HCO_3	45	8.1	7.3	-103.0	-14.2	8.8	3.4	1.4	1.7	<2	9.8	[2.1]	[1.6]	[0.0]	[0.3]	14.3	[0.1]	0.0	<0.0	[5]	<1	n.m.
S-16	30322	200476	2056	Ca-Mg-Na-SO_4-HCO_3	56	4.8	7.3	-105.9	-14.5	8.5	4.5	1.5	2.1	<2	10.4	[2.1]	[1.6]	[0.0]	[0.3]	16.9	<0.2	[0.0]	<0.0	[5]	<1	n.m.
S-17	32195	200407	2152	Ca-Mg-SO_4	170	2.5	7.8	-103.8	-14.3	8.6	20.8	4.8	1.9	[1.5]	6.7	[2.0]	[1.1]	0.0	<0.1	76.7	0.1	<0.0	<0.0	<0.0	[0.7]	[0.3]
S-18	30604	200164	1907	Ca-SO_4	78	1.2	7.6	-106.1	-14.4	8.1	8.3	1.4	1.9	[1.5]	7.9	[2.0]	[1.1]	0.0	[0.0]	25.5	0.1	0.0	<0.0	[0.0]	[0.7]	[0.1]
S-19	31797	199981	2008	Ca-Mg-SO_4	110	3.4	7.8	-104.6	-14.2	7.9	11.1	2.8	2.3	[1.5]	10.4	[2.0]	[1.1]	0.0	0.1	35.1	0.1	<0.0	<0.0	<0.0	[0.7]	[0.3]
S-20	31927	199775	2072	Ca-Mg-SO_4	591	6.4	7.3	-95.9	-13.3	9.6	87.4	23.8	3.1	3.0	15.9	[2.1]	[1.6]	[0.0]	[0.3]	293.2	[0.1]	0.2	<0.0	[5]	<1	n.m.
S-21	32465	199058	2350	Ca-Mg-SO_4	693	3.4	7.4	-103.4	-14.3	n.m.	95.5	23.8	3.5	2.3	9.2	[2.0]	<1.6	<0.0	[0.0]	316.5	0.1	[0.0]	<0.0	[0.0]	[0.6]	<1
S-22	33005	198717	2481	Ca-Mg-SO_4	1399	1.8	7.0	-104.5	-14.5	n.m.	204.4	65.2	4.5	3.6	8.5	[2.0]	<1.6	<0.0	0.1	766.0	0.1	[0.0]	<0.0	[0.0]	[0.6]	[0.1]
S-23	29282	198701	2169	Ca-HCO_3	61	2.1	7.9	-99.7	-13.6	8.8	9.1	[0.9]	[1.0]	[1.5]	28.7	[2.0]	<1.6	<0.0	[0.0]	5.4	0.1	0.0	<0.0	[0.0]	[0.7]	16.2
S-24	31566	198680	1968	Ca-SO_4	333	4.9	7.3	-100.9	-13.7	n.m.	44.3	6.6	3.5	<2.2	20.1	[2.0]	[1.1]	<0.0	[0.0]	177.5	0.2	<0.0	<0.0	[0.0]	[0.6]	<1
S-25	31598	198191	2100	Ca-SO_4	446	4.5	7.8	-99.6	-13.7	8.4	65.2	10.0	4.0	2.1	16.5	[2.1]	[1.6]	0.0	[0.3]	197.3	[0.1]	0.2	<0.0	[5]	<1	n.m.
S-26	31457	196642	2069	Ca-SO_4-HCO_3	129	1.5	8.5	-103.0	-14.2	9.0	17.0	1.5	1.7	[1.5]	15.3	[2.0]	<1.6	0.0	[0.0]	41.8	0.2	0.0	<0.0	<0.0	[0.7]	1.7
S-27	31072	196280	1872	Ca-Na-SO_4-HCO_3	87	3.5	7.8	-97.0	-13.4	7.4	8.8	<1.3	4.6	[1.5]	16.5	[2.0]	2.6	[0.0]	[0.0]	21.7	0.6	0.1	<0.0	[0.0]	[0.7]	8.5
S-28	31043	195789	1920	Ca-SO_4-HCO_3	40	3.3	7.2	-95.4	-13.0	8.0	3.6	<1.3	<1.5	[1.5]	6.7	[2.0]	3.7	<0.0	[0.0]	8.4	0.1	[0.0]	<0.0	[0.0]	[0.7]	[0.1]
S-29	31450	195773	2204	Ca-Mg-SO_4	128	2.8	7.0	-104.5	-14.4	10.8	11.5	3.5	1.1	<2	4.9	[1.6]	[1.5]	[0.0]	[0.1]	43.9	[0.1]	[0.0]	<0.0	[5]	<1	<1
S-30	32007	195690	2468	Ca-Mg-SO_4	187	3.5	7.2	-101.2	-14.0	9.7	19.7	6.1	2.1	<2	3.7	[2.1]	[1.6]	[0.0]	[0.3]	76.2	[0.1]	[0.0]	<0.0	[5]	<1	n.m.
S-31	31205	195317	2053	Ca-HCO_3-SO_4	127	0.5	7.9	-98.6	-13.5	7.9	15.9	2.1	<1.5	[1.5]	45.8	[2.0]	[1.1]	0.0	[0.0]	14.3	0.1	0.1	<0.0	[0.0]	[0.7]	[0.1]
S-32	30340	195310	1968	Ca-Mg-SO_4-HCO_3	73	2.8	7.5	-97.6	-13.5	8.9	7.7	1.7	<1.5	[1.5]	8.5	[2.0]	[1.1]	<0.0	[0.0]	22.7	0.1	[0.0]	<0.0	[0.0]	[0.7]	[0.1]
S-33	29988	194900	2252	Ca-SO_4-HCO_3	26	1.9	7.7	-97.8	-13.3	8.0	2.2	[0.9]	[1.0]	[1.5]	6.7	[2.0]	[1.1]	[0.0]	[0.0]	5.5	0.1	<0.0	<0.0	[0.0]	[0.7]	[0.1]

Table 2: Selected examples of the chemistry of the spring waters (i.e. samples with the highest EC values). <'value'… measured content below the limit of determination; ['value']… measured content below the limit of detection; n.m…. parameter not measured. Water type is defined by major cations and anions with %meq/l concentrations ≥ 20 % in descending order according to their concentrations and where concentrations are ≥ 50 % the corresponding ion is underlined (e.g. Ca-Mg-SO_4-HCO_3).

Sample	X-Coord.	Y-Coord.	Altitude [m.asl]	Water-Type	EC [µS/cm]	T [°C]	pH	^{2}H [‰]	^{18}O [‰]	^{3}H [TU]	Ca [mg/l]	Mg [mg/l]	Na [mg/l]	K [mg/l]	HCO_3 [mg/l]	Cl [mg/l]	NO_3 [mg/l]	NO_2 [mg/l]	o-PO_4 [mg/l]	SO_4 [mg/l]	F [mg/l]	NH_4 [mg/l]	Fe [mg/l]	Mn [µg/l]	Sb [µg/l]	As [µg/l]	Al [mg/l]
DW-01	31387	201811	1785	Ca-Mg-SO_4-HCO_3	310	10.5	9.5	-105.8	-14.3	7.4	34.0	7.2	3.3	4.6	43.3	[1.8]	< 1.2	0.0	[0.1]	102.3	< 0.1	0.1	< 0.0	< 1	n.m.	n.m.	n.m.
DW-02	31388	201810	1785	Ca-Mg-SO_4	283	4.6	8.0	-105.7	-14.2	6.9	29.3	7.2	2.1	3.8	12.8	[1.8]	< 1.2	0.0	[0.1]	97.5	[0.1]	[0.0]	< 0.0	< 1	n.m.	n.m.	n.m.
DW-03	31404	201797	1787	Ca-Mg-SO_4	263	3.3	7.6	-105.8	-14.5	n.m.	28.9	6.8	1.7	< 2	9.8	[1.5]	[1.3]	<0.0	[0.0]	87.9	< 0.1	0.2	< 0.0	1.3	n.m.	n.m.	n.m.
DW-04	31411	201791	1788	Ca-Mg-SO_4	247	4.0	8.6	-106.1	-14.4	n.m.	31.6	8.3	2.1	< 2	22.0	[1.5]	[1.3]	[0.0]	0.0	87.4	[0.1]	[0.0]	0.0	3.2	n.m.	n.m.	n.m.
DW-05	31418	201785	1790	Ca-Mg-SO_4	230	3.8	8.3	-106.5	-14.6	n.m.	29.9	6.3	2.4	< 2	12.8	[1.5]	[1.3]	[0.0]	< 0.0	84.7	< 0.1	[0.0]	< 0.0	< 1	n.m.	n.m.	n.m.
DW-06	31441	201767	1791	Ca-SO_4	259	4.6	8.3	n.m.	n.m.	n.m.	27.5	4.4	3.3	2.3	23.2	6.8	[1.3]	0.0	< 0.0	81.5	[0.1]	0.2	0.0	61.8	n.m.	n.m.	n.m.
DW-07	31562	201733	1796	Ca-HCO_3-SO_4	290	n.m.	11.3	-108.4	-14.8	n.m.	36.6	< 1	10.0	18.0	103.7	[1.5]	[1.3]	0.0	[0.0]	62.3	0.4	1.9	< 0.0	< 1	n.m.	n.m.	n.m.
DW-08	31562	201733	1796	Ca-SO_4	178	5.1	8.5	-108.5	-14.8	8.6	22.9	3.3	3.1	2.5	19.5	<2.2	[1.3]	[0.0]	[0.0]	63.8	0.3	0.3	< 0.0	58.5	n.m.	n.m.	n.m.
DW-09	31562	201733	1796	Ca-SO_4-HCO_3	179	5.3	8.5	-109.5	-14.9	9.6	22.7	3.1	3.3	2.7	36.0	[1.5]	[1.3]	0.0	< 0.0	58.4	0.4	1.3	0.0	16.8	n.m.	n.m.	n.m.
DW-10	31562	201733	1796	Ca-SO_4-HCO_3	211	6.6	8.9	-109.3	-14.9	8.6	22.6	3.1	4.0	2.8	28.7	[1.5]	11.8	0.0	< 0.0	59.3	0.4	3.2	< 0.0	17.3	n.m.	n.m.	n.m.
DW-11	31385	201813	1785	Ca-Mg-SO_4	211	3.7	9.2	-115.4	-15.4	8.9	25.9	6.5	1.9	< 2	15.9	[1.4]	[1.8]	[0.0]	[0.0]	82.4	[0.1]	[0.0]	< 0.0	< 1	n.m.	n.m.	n.m.
DW-12	31430	201779	1791	Ca-Mg-SO_4	341	5.2	7.3	n.m.	n.m.	n.m.	30.2	6.6	2.3	2.6	14.0	< 1	0.8	0.0	< 0.0	81.9	< 0.1	<0.0	< 0.0	20.9	n.m.	n.m.	n.m.
DW-13	31430	201779	1791	Ca-Mg-SO_4-HCO_3	282	4.4	7.6	n.m.	n.m.	n.m.	29.5	6.2	2.5	< 2	37.8	< 1	0.6	0.0	< 0.0	74.1	< 0.1	0.0	< 0.0	2.8	n.m.	n.m.	n.m.
DW-14	31433	201775	1791	Ca-SO_4	268	8.1	9.3	n.m	n.m.	n.m.	36.3	4.7	3.4	4.7	12.2	1.8	0.4	0.1	0.1	76.5	0.2	0.4	< 0.0	12.4	n.m.	n.m.	n.m.
DW-15	31430	201779	1791	Ca-Mg-SO_4	236	4.5	7.6	n.m	n.m.	n.m.	30.6	6.0	2.6	< 2	18.3	< 1	0.6	<0.0	< 0.0	73.2	0.1	[0.0]	< 0.0	< 1	n.m.	n.m.	n.m.
DW-16	31433	201775	1791	Ca-SO_4-HCO_3	245	8.0	7.8	n.m	n.m.	n.m.	36.7	6.0	2.7	2.2	30.5	< 1	0.4	0.0	< 0.0	82.7	0.3	[0.0]	< 0.0	1.4	n.m.	n.m.	n.m.
DW-17	31443	201433	1815	Ca-Mg-SO_4	233	3.9	7.5	n.m	n.m.	n.m.	26.5	9.6	3.6	2.1	4.3	< 1	1.1	n.m.	n.m.	102.0	0.2	n.m.	0.0	< 5	< 1	7.4	0.0
DW-18	31536	201433	1808	Ca-Mg-SO_4	214	5.1	6.3	n.m	n.m.	n.m.	17.9	6.8	8.3	4.4	9.8	< 1	< 1	n.m.	n.m.	85.4	1.4	n.m.	< 0.0	5.2	< 1	< 1	0.1
DW-19	31562	201725	1797	Ca-SO_4-HCO_3	228	5.5	7.1	n.m	n.m.	n.m.	30.7	4.3	4.3	3.0	32.3	< 1	< 1	n.m.	n.m.	80.0	0.5	n.m.	< 0.0	< 5	< 1	2.1	< 0.0
DW-20	31562	201728	1797	Ca-SO_4-HCO_3	228	5.4	7.3	n.m	n.m.	n.m.	31.0	4.3	4.3	3.1	32.9	< 1	< 1	n.m.	n.m.	80.1	0.4	n.m.	< 0.0	< 5	< 1	1.3	< 0.0
DW-21	31430	201779	1791	Ca-Mg-SO_4	273	4.2	6.5	n.m	n.m.	n.m.	36.0	7.5	2.6	2.1	11.0	< 1	< 1	n.m.	n.m.	119.0	0.1	n.m.	< 0.0	< 5	< 1	< 1	< 0.0
DW-22	31384	201814	1785	Ca-Mg-SO_4	299	3.6	6.4	n.m.	n.m.	n.m.	36.0	10.7	1.9	1.9	7.9	< 1	< 1	n.m.	n.m.	134.0	<0.1	n.m.	< 0.0	< 5	< 1	< 1	< 0.0
DW-23	31562	201471	1805	Ca-Mg-SO_4	207	5.1	6.8	n.m.	n.m.	n.m.	19.8	5.2	8.7	3.9	21.4	< 1	< 1	n.m.	n.m.	71.1	2.4	n.m.	< 0.0	< 5	< 1	< 1	< 0.0
DW-24	34038	200129	1766	Ca-Na-HCO_3-SO_4	190	7.8	8.1	-113.5	-15.1	n.m.	23.4	< 1	10.2	< 2	59.8	[1.8]	[1.5]	[0.0]	[0.1]	46.4	1.0	0.1	< 0.0	<20	< 1	15	n.m
DW-25	33721	200038	1765	Ca-Na-SO_4-HCO_3	244	7.2	7.9	-109.4	-14.7	n.m.	29.2	1.8	12.4	< 2	67.1	[1.8]	[1.5]	[0.0]	[0.1]	62.3	1.9	0.1	< 0.0	<20	< 1	1.7	n.m.
DW-26	33384	199941	1763	Ca-SO_4-HCO_3	290	5.6	7.4	-102.5	-13.8	n.m.	43.3	4.1	2.6	< 2	62.2	[1.8]	[1.5]	[0.0]	[0.1]	82.8	0.3	<0.1	< 0.0	[5]	< 1	1.1	n.m.
DW-27	28665	196953	1765	Ca-Na-HCO_3-SO_4	149	14.6	7.9	-106.4	-14.5	n.m.	16.5	1.2	9.0	< 2	51.9	[1.8]	[1.5]	[0.0]	[0.1]	26.1	2.3	[0.0]	< 0.0	[5]	< 1	116.0	n.m.
DW-28	29139	197028	1764	Ca-Na-HCO_3-SO_4	173	14.2	8.0	-91.9	-12.6	n.m.	20.7	< 1	9.9	< 2	61.6	[1.8]	[1.5]	[0.0]	[0.1]	30.6	2.4	[0.0]	< 0.0	[5]	< 1	95.1	n.m.

Table 3: Selected examples of the chemistry of the tunnel inflow waters (i.e. samples with the highest EC values). <'value'... measured content below the limit of determination; ['value']... measured content below the limit of detection; n.m.... parameter not measured. Water type is defined by major cations and anions with %meq/l concentrations ≥ 20 % in descending order according to their concentrations and where concentrations are ≥ 50 % the corresponding ion is underlined (e.g. Ca-Mg-SO_4-HCO_3).

are the SO_4/HCO_3 and Ca/Mg ratios, which are slightly lower in the Klasgarten Drift than in the surrounding springs. The samples from the water inflows from within the conduction galleries DW-24, DW-25, DW-26, DW-27 and DW-28 have generally higher amounts of Na and HCO_3 in comparison to the other groundwaters with the exception of DW-26. Some of the water inflows in the drift and conduction galleries contain high amounts of As, Mn and Ni (Table 3).

The EC of the spring and tunnel inflow waters increases with increasing Ca, Mg and SO_4 concentrations but not with HCO_3 (Figures 5 and 6). This indicates that the dominant cations Ca and Mg are mostly balanced by SO_4 and not by HCO_3. Furthermore, a general increase in Mg with increasing Ca concentration is evident indicating a link between the dissolution of Ca- and Mg-bearing minerals. In contrast, there is no distinct correlation between Ca (or any other analysed cation) and HCO_3 (Figure 6 d). No clear trend between the EC and Na or K is present.

The cross correlation diagrams (Figure 6) indicate a strong linear correlation between Ca+Mg and SO_4 with a molar (Ca+Mg)/SO_4 ratio of 1 and a molar Ca/SO_4 ratio between 0.67 and 1 for the majority of the samples. These waters contain significantly higher amounts of total dissolved solids than waters with a molar Ca/SO_4 ratio of more than 1. HCO_3 is present in rather low concentrations of approximately 5-20 mg/l in most springs and higher concentrations of approximately 20-50 mg/l in most tunnel inflow waters.

According to calculations using PHREEQC Interactive

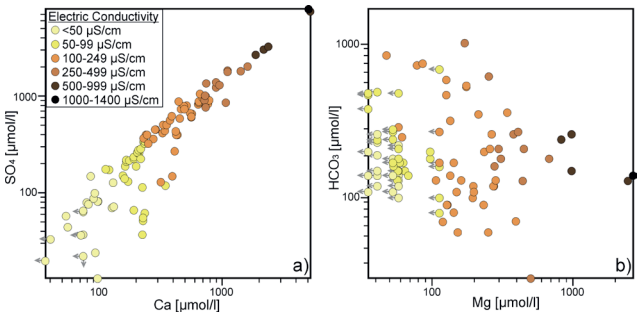

Figure 5: Log-log plot of Ca vs. SO_4 (a) and Mg vs. HCO_3 (b) for all analysed spring (n = 101) and tunnel inflow (n = 28) samples. The samples are also differentiated according to their EC values. Symbols marked with arrows indicate that their concentration is below the limit of detection for one or both parameters.

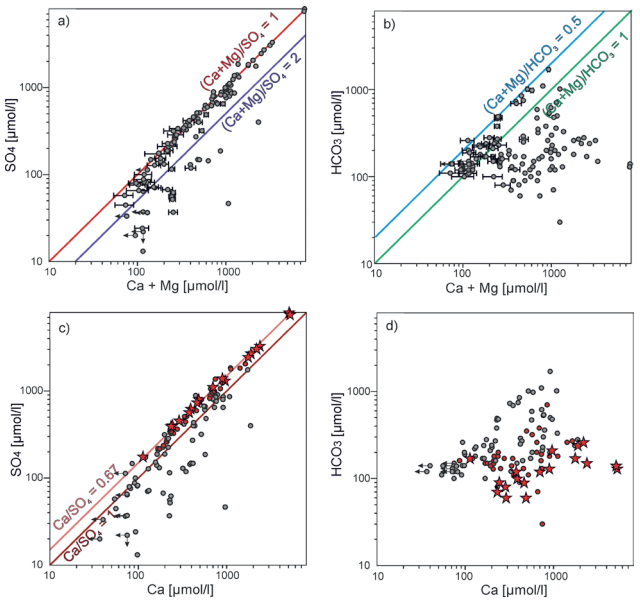

Figure 6: Log-log plots of Ca + Mg vs. a) SO_4 and b) HCO_3 and c) of Ca vs. c) SO_4 and d) HCO_3 of all the water samples (n = 129). Arrows and uncertainty bars indicate samples where the parameters are below the limit of detection in one or both directions. Ratios of end members, as described in text, are depicted in a) and b). Samples with a (Ca+Mg)/SO_4 ratio of 1 (±10%) are highlighted red in c) and d). Samples with a Ca:Mg:SO_4 ratio of 2:1:3 (±10%) are marked by a red star.

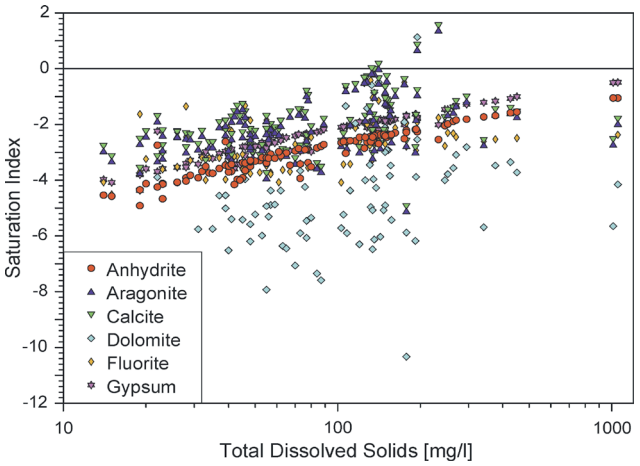

Figure 7: Saturation indices for various minerals of the analysed groundwater samples (n = 127).

only a few samples from the Klasgarten Drift are saturated with respect to carbonate minerals (Figure 7). All other water samples were below the saturation index (SI) for calcite, aragonite, dolomite, gypsum and anhydrite (SI < 0). There is no clear trend between the SI for carbonates and the amount of total dissolved solids. The SI of gypsum and anhydrite increases logarithmically with the amount of total dissolved solids. This indicates only one main dissolution process which gives rise to the chemical composition of these waters.

Sample DW-14 was the only one which was saturated with respect to hydroxyapatite, but the occurrence of phosphates in the field has not yet been validated.

5.2 Oxygen and hydrogen isotopes

At the beginning of the 1950s, before the atmospheric nuclear bomb tests, the natural Tritium content of precipitation was about 5 TU (Roether, 1967). By the year 1963, the Tritium content of precipitation had greatly increased to over 2000 TU as a result of the nuclear tests (Clark and Fritz, 1997). Since 1964, there has been an approximately exponential decay of the Tritium content in precipitation. This means that it has been possible to estimate the mean residence time of groundwater (<100 years) due to the rise or fall of the measured Tritium content (Clark and Fritz, 1997; Mazor, 2003). However, the interpretation of Tritium values obtained from groundwater has become increasingly difficult due to the flattening of the time versus radioactive decay curves in the last 20 years.

Figure 8 depicts the curves of the weighted Tritium values from precipitation stations close to the study area and the values obtained from the groundwater within the study area between 2009 and 2011. The data indicate short residence times of <5 years for the groundwater as recent precipitation (2007-2010) has an annually weighted value of 8-10 TU (Figure 8; Kralik, 2015).

Further, the monthly Tritium values of the springs fluctuated between approximately 7 and 11 TU during the observation periods and show, like the monthly Tritium values of precipitation (Reutte 2.7-16.9 TU and Längenfeld 2.3-15.5 TU for the periods January 2000 to December 2002 and January 2007 to September 2010, respectively), large, seasonal variations. This indicates that Tritium is not completely buffered or mixed over long periods of time while the waters circulate through the aquifers. Further, there is no correlation between Tritium and any ion concentration indicating that the measured Tritium values are not attributable to a mixture of young (8-15 TU) and older water (<2 TU).

Additionally, the seasonal $\delta^{18}O$ values in precipitation follow a sinusoidal curve (Figure 9). In very young groundwater this $\delta^{18}O$ curve is observed albeit attenuated and phase-shifted. This effect allows the calculation of the mean residence times of up to five years for shallow groundwater and karst water in accordance with the exponential model of Stichler and Herrmann (1983; see also Mook, 2000).

For the springs shown in Figure 9, the following mean re-

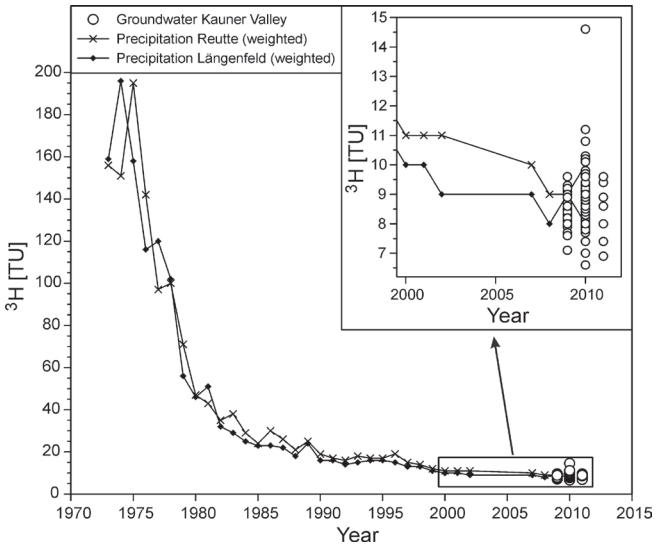

Figure 8: Plot of all Tritium values (n = 99) obtained from the springs and tunnel inflow waters in the Kauner Valley in relation to the yearly weighted averages values of Tritium from precipitation obtained from weather stations at Längenfeld and Reutte. The Längenfeld station in the Ötz Valley is located some 25 km to the east of the studyarea. The Reutte station is some 55 km to the north. The one outlier plotting at 14.6 TU comes from spring S-25 where the other four values obtained lie between 8.2 and 9.3 TU. The inset in the top right corner is a detail view for the period 2000-2011. The raw Tritium precipitation data was obtained from the Environment Agency Austria Website (www.umweltbundesamt.at/umweltsituation/wasser/isotopen/isotopen) Data sources: Umweltbundesamt GmbH, ARC-Seibersdorf/GSFMünchen; ANIP – Austrian Network for Isotopes in Precipitation.

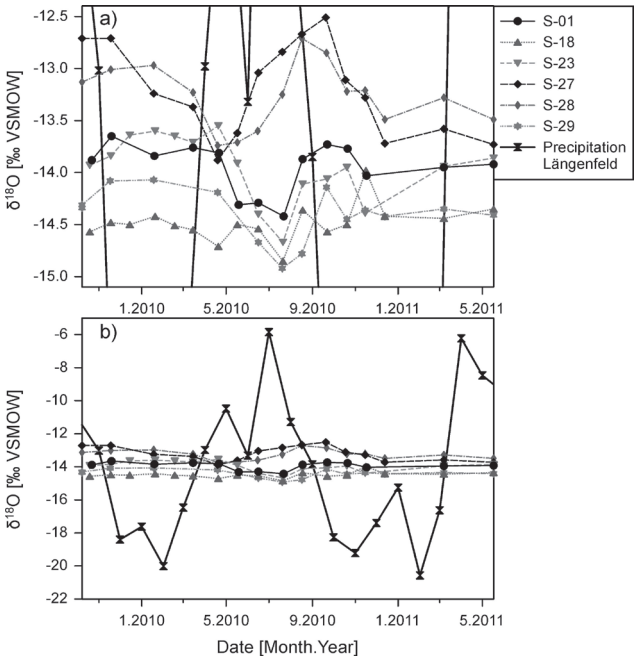

Figure 9: Seasonal variation of δ^{18}O in precipitation at Längenfeld and in the springs S-01, S-18, S-23, S-27, S-28 and S-29 between October 2009 and May 2011; (a) y-axis adjusted to the amplitude of the δ^{18}O values of the spring water; (b) y-axis adjusted to the amplitude of the δ^{18}O values in precipitation.

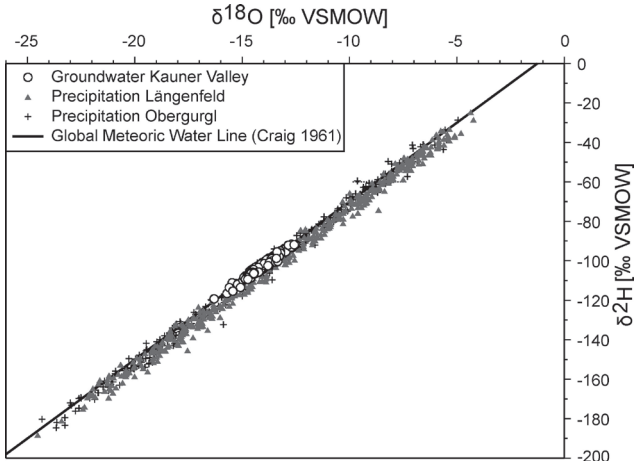

Figure 10: Plot of δ^{18}O vs δ^2H. Depicted are all (n = 275) δ^{18}O and δ^2H values obtained from the springs and tunnel inflow waters in the Kauner Valley. Also shown are the δ^{18}O and δ^2H values of monthy precipitation (n = 703) obtained from the weather stations at Obergurgl and Längenfeld in the Ötz Valley located some 25 km to the east of the study area. The precipitation values represent the period 1973 to 2011. The raw precipitation data was obtained from the Environment Agency Austria Website (www.umweltbundesamt.at/umweltsituation/wasser/isotopen/isotopen) Data sources: Umweltbundesamt GmbH, ARC-Seibersdorf/GSFMünchen; ANIP – Austrian Network for Isotopes in Precipitation.

sidence times using the exponential model of Stichler and Herrmann (1983) were calculated: S-01: 3.4 yrs., S-18: 2.6 yrs., S-23: 2.0 yrs., S-27: 1.6 yrs., S-28: 2.2 yrs. and S-29: 2.6 yrs. These springs were considered for calculation as they had the largest number of data available (14 to 17 monthly measurements each). For the precipitation input values, a four year period from January 2007 to December 2010 from the weather station Längenfeld was used.

Lastly, the δ^{18}O and δ^2H values obtained from the groundwater from the study area fall on the Global Meteoric Water Line (Craig, 1961) and indicate that no fractionation process (e.g. evaporation) has taken place and that the investigated groundwater is of meteoric origin. Consequently, the high values of total dissolved solids are not caused by evaporation or geothermal processes (>80°C, Mook, 2000) (Figure 10).

5.3 Sulphur isotopes

Sulphur isotopes of four spring water samples with high sulphate concentrations were analysed to trace the origin of the dissolved sulphate. The δ^{34}S values of +0.6 to +6.2 ‰ VCDT can be considered low (Table 4). Given that the δ^{34}S value depends on fractionation processes during mineral formation, organically-bound sulphur and reduced sulphur of sulphide (e.g. pyrite, sphalerite) are depleted in ^{34}S as known from sulphides in the investigation area (δ^{34}S ≈ 0 ‰ VCDT; Vavtar, 1979; cf. Chapter 3.2 Ore deposits) and from pyrite porphyroblasts with δ^{34}S values between +1.9 and +5.3 ‰ VCDT analysed from quarzitic schists of the Glockner and Venediger Nappes within the Tauern Window, Wipp Valley area, Tyrol, some 60 km to the east of the study area (Millen and Spötl, unpubl. report 2006).

In Tyrol, marine evaporites have δ^{34}S values between +10 and +27 ‰ VCDT (Spötl, 1988 a, b and c; Spötl and Pak,

Spring	EC [µS/cm]	pH	Ca [mg/l]	Mg [mg/l]	HCO_3 [mg/l]	SO_4 [mg/l]	$\delta^{34}S$ [‰]
S-10	142	6.3	28.1	9.73	7.3	107	2.9
S-12	142	6.4	29.2	6.18	11.6	95.7	4.5
S-20	302	6.4	70.3	18.5	10.4	236	6.2
S-22	705	6.3	210	59.7	7.9	722	0.6

Table 4: Selected major ions, EC, pH and $\delta^{34}S$ values of spring waters.

1996; Götzinger et al., 2001; Millen and Brandner, 2001; Spötl et al., 2002; Millen et al., 2003; Mittermayr et al., 2012). Consequently, the oxidation of sulphides releases dissolved sulphate with lower $\delta^{34}S$ values than the dissolution of marine evaporites.

6. Discussion

6.1 Possible water-rock interactions

The Tritium and $\delta^{18}O$ data indicate residence times of the groundwater of <5 years. It can therefore be assumed that the bulk of the dissolved solids in the groundwater does not originate from the bedrock, which consists of highly insoluble silicates (e.g. quartz, feldspar, mica, amphibole), but from the dissolution of accessory minerals such as carbonates, sulphides and, if present, sulphates, whose dissolution rates are much higher than those of silicates (Matthess, 1994; Tóth, 1999; Kilchmann, 2001).

A simple explanation of the observed ratio of 1 for $(Ca+Mg)/SO_4$ would be the dissolution of sulphate minerals, for example, the dissolution of gypsum:

$$CaSO_4 \cdot 2H_2O \leftrightarrow Ca^{2+} + SO_4^{2-} + 2H_2O$$

However, the measured $\delta^{34}S$ values (+0.6 to +6.2 ‰ VCDT) indicate that sulphate in the spring waters originates from the oxidation of sulphides (cf. Chapter 5.3 Sulphur isotopes). A mixing of two different water types with both low and high $\delta^{34}S$ values can essentially be ruled out since the sample with the highest sulphate concentration is characterised by the lowest $\delta^{34}S$ value (Table 4). This is in accordance with the field studies showing no evidence of gypsum in the study area. However, highly mineralised groundwater, which has become saturated with respect to gypsum, could result in localised precipitation of secondary gypsum along fractures. The only indication for the occurrence of this process was the observation of secondary gypsum a few kilometres north of the study area (Bernhard, 2008; cf. Chapter 3.3 Fracture minerals).

The dissolution of carbonates and the oxidation of pyrite are regarded as the most plausible processes responsible for producing the highly mineralised water in the aquifers of the study area as in many other crystalline aquifers in Tyrol and the Alps in general (e.g. Millen, 2003; Kilchmann et al., 2004; Sacchi et al., 2004; Madritsch and Millen, 2007). These processes are strongly controlled by microbial activity and are favoured at low pH-values. As a secondary product, Fe-oxides and Fe-hydroxides precipitate along the water flow paths resulting in reddish brown fracture coatings (cf. Chapter 3.2 Ore deposits and Chapter 3.3 Fracture minerals, Figure 3).

The products of these processes depend on the behaviour of CO_2 during the neutralisation. If CO_2 remains in the system (i.e. no ongoing exchange with the atmosphere) water interacts with carbonate minerals and pyrite in a closed system according to the following reactions:

$$2FeS_2+8Ca(CO_3)_2+7.5O_2+7H_2O \leftrightarrow 2Fe(OH)_3+8Ca^{2+}+4SO_4^{2-}+8HCO_3^-$$

for calcite dissolution and

$$2FeS_2+4CaMg(CO_3)_2+7.5O_2+7H_2O \leftrightarrow 2Fe(OH)_3+4Ca^{2+}+4Mg^{2+}+4SO_4^{2-}+8HCO_3^-$$

for dolomite dissolution. This results in a $(Ca+Mg)/SO_4$ ratio of 2 and a $(Ca+Mg)/HCO_3$ ratio of 1.

In contrast, the dissolution of carbonates and the oxidation of pyrite in an open system (e.g. Cravotta et al., 1990) result in a molar $(Ca+Mg)/SO_4$ ratio of 1 according to:

$$2FeS_2+4CaCO_3+7.5O_2+3H_2O \leftrightarrow 2Fe(OH)_3+4Ca^{2+}+4SO_4^{2-}+4CO_2$$

for calcite dissolution and

$$2FeS_2+2CaMg(CO_3)_2+7.5O_2+3H_2O \leftrightarrow 2Fe(OH)_3+2Ca^{2+}+2Mg^{2+}+4SO_4^{2-}+4CO_2$$

for dolomite dissolution, respectively. These reactions assume that CO_2 degasses into the atmosphere.

The majority of the water samples in the study area are characterised by a $(Ca+Mg)/SO_4$ ratio between 1 and 2 (Figure 6 a), but predominantly close to 1 (Figure 6 c, highlighted in red). This indicates a mixing of waters dominated by carbonate dissolution and pyrite oxidation in both open and closed systems, dominantly, however, in an open system. This is also indicated by the fact that there is hardly any correlation between Ca+Mg and HCO_3 and Ca and HCO_3 for the majority of the samples (Figure 6 b and d). However, HCO_3 must be produced to provide the measured levels of alkalinity.

In addition to the oxidation of sulphides, dissolution of carbonates can also occur via carbonic acid digestion according to these reactions:

$$CaCO_3+H_2O+CO_2 \leftrightarrow Ca^{2+}+2HCO_3^-$$

$$CaMg(CO_3)_2+2H_2O+2CO_2 \leftrightarrow Ca^{2+}+Mg^{2+}+4HCO_3^-$$

which lead to a $(Ca+Mg)/HCO_3$ ratio of 0.5 in the groundwater. These reactions play a role where soil formation in the catchment is significant, i.e. below the timberline (Figure 6 b). Several samples indicate a mixing of carbonate dissolution by CO_2 which originates from soil, and carbonate dissolution by sulphide oxidation.

Cation/sulphate ratio	Spring and tunnel water inflows
$(Ca+Mg)/SO_4 = 1$ ±10 %	S-03, S-04, S-06, S-07, S-08, S-12, S-14, S-15, S-16, S-17, S-18, S-19, S-21, S-25, S-32, DW-1, DW-2, DW-3, DW-6, DW-8, DW-11, DW-17, DW-21, DW-23
$Ca:Mg:SO_4 = 2:1:3$ ±10 %	S-10, S-11, S-13, S-20, S-22, S-25, S-29, S-30, DW-22
$(Ca+Mg)/SO_4 \neq 1$ $Ca:Mg:SO_4 \neq 2:1:3$ ±10 %	S-01, S-02, S-05, S-09, S-23, S-24, S-26, S-27, S-28, S-31, S-33, DW-4, DW-5, DW-7, DW-9, DW-10, DW-12, DW-13, DW-14, DW-15, DW-16, DW-18, DW-19, DW-20, DW-24, DW-25, DW-26, DW-27, DW-28

Table 5: Molar cation/sulphate ratios for spring and tunnel water inflows based on the cross analysis of the elements as given in Figure 6. For the locations of the sampling points see Figure 1. Water samples which do not fit the ratio criteria still obtained their composition mainly from the dissolution and oxidation processes discussed in chapter 6.1 Possible water-rock interactions.

A number of samples are characterised by a $Ca:Mg:SO_4$ ratio of 2:1:3 (Figure 6 c, highlighted as stars) indicating dissolution of more calcite than dolomite and/or other carbonates, such as ankerite, $Ca(Fe,Mg,Mn)(CO_3)_2$.

Dissolution of silicates with a Ca/Mg ratio of 2 might also be considered, but no silicates of such a composition were found in the study area. Silicate dissolution associated with high sulphate concentrations can be mediated by geomicrobiological processes according to laboratory-based investigations (Ehrlich, 1998; Sonnleitner et al., 2011). According to these studies, bacterial oxidation of sulphur results in a decrease of the pH-value and silicates such as feldspar and phyllosilicates may be dissolved more easily. This kind of dissolution usually occurs incongruently (Ehrlich, 1998) and buffers the pH-value. A combined increase of Ca, Mg and SO_4 in metamorphic rocks was measured in laboratory tests by Sonnleitner et al. (2011). Given that plagioclase, amphiboles and chlorites in the study area are characterised by significantly different cation ratios (Zangerl, 1997; Strauhal, 2009) this process most probably plays only a minor role in the study area.

The source of Na and K could either be the presence of NaCl in fluid inclusions, ion exchange or the incongruent dissolution of silicates such as feldspars or micas. For example, Selverstone et al. (1995) reported the existence of NaCl-rich fluid inclusions in the Obere Schieferhülle of the Glockner Nappe (~6.5 wt% NaCl) and the Central Gneiss (~10 wt% NaCl) of the Tauern Window, Tyrol. The detection limits for Cl in this study were too high (Tables 2 and 3) to measure this element and assess these processes.

Fluoride most probably originates from biotite and localised anomalies of trace elements (e.g. As and Mn) in some of the spring and tunnel waters (e.g. S-23 and S-08) likely originate from dissolution of ore minerals (e.g. arsenopyrite and Mn-rich siderite; cf. Schroll 1997; cf. 3.2 Ore deposits).

6.2 Possible influence of rock deformation on water-rock interactions

Combining the hydrochemical data with the lithological information reveals that a $(Ca+Mg)/SO_4$ ratio of 1 ±10% (cf. Figures 1 and 6 and Table 5) is typical of waters emerging from areas consisting mainly of fractured paragneiss and deposits made up thereof, i.e. rockslide, debris, and talus deposits. The chemistry of some of the water samples from within the Klasgarten Exploration Drift with a similar ratio indicates that air locally circulates down to great depths within the rockslide (see discussion below). A $Ca:Mg:SO_4$ ratio of 2:1:3 ±10% is observed at some springs emerging at the mouths of high altitude tributary valleys as well as at one tunnel inflow in the Klasgarten Drift (depicted as red stars in Figures 1 and 6). The chemistry of waters which do not follow either of these trends (depicted in grey in Figures 1 and 6) are typical of areas dominated by a) orthogneiss and/or b) bedrock that is hardly fractured and c) from water taken from within the deep lying water conduction galleries (cf. Table 5). Also the values from S-09 spring water, which is characterised by low amounts of total dissolved solids, do not follow these trends.

Given that the hydrochemical analyses (cf. Chapter 6.1 Possible water-rock interactions) strongly suggest that carbonate dissolution and sulphide oxidation in an open system requires the contact of the water with the atmosphere, this process can also be related to the deformation behaviour and current fragmentation of the bedrock and the resulting subsurface ventilation to more than 100 m within the rockslides (cf. Chapter 3.4 Quaternary deposits).

The paragneiss in the study area is characterised by a higher fracture density than the orthogneiss. Further, due to its lower rock mass strength, paragneiss is more prone to deep-seated gravitational deformation, hence rockslides preferentially develop in this lithology (Zangerl et al., 2010). As a result of the intense disintegration of the rock mass to more than 100 m of depth during rockslide development, water circulating through these deposits contains elevated sulphate concentrations, although pyrite and other sulphides are only present as accessory minerals. Further, with increased subsurface ventilation, pyrite oxidation and sulphate formation speed up (cf. Deutsch, 1997).

Elevated amounts of total dissolved solids are also present in waters emerging from melting permafrost and rock glacier ice, similar to the observations by Thies et al. (2013).

6.3 Comparison with regional case studies in the Alps

This study's finding – the prevalence of $Ca\text{-}Mg\text{-}SO_4$ type groundwater – is inconsistent with the Hydrochemical Map of Austria (Kralik et al., 2005) which indicates that $Ca\text{-}HCO_3$ type groundwater dominates the silicate rock aquifers of the study area.

Nevertheless, the link between water chemistry and litho-

logy, as proposed in this study, is in agreement with hydrochemical investigations of nearby regions. For example, in several locations in the southern Kauner Valley (Krumgampen Valley) and the southern Ötz Valley (Hochebenkar; Thies et al., 2013) the streams draining fragmented, paragneiss-dominated catchments (according to Hammer, 1923 b) have a stoichiometric $(Ca+Mg)/SO_4$ ratio of 1, whereas streams from amphibolite catchments (according to Hammer, 1923 b) show a different chemical composition (Thies et al., 2013: listed as KG-R1, KG-R2 and KG-R3). Springs emerging from tectonised gneisses along deep-seated mass movements at the southern fringe of the Ötztal-Stubai Basement Complex also show high EC values and classify as $Ca\text{-}Mg\text{-}HCO_3\text{-}SO_4$ type groundwater (Spötl et al., 2002).

Carbonate fracture fillings in silicate rocks have also been described e.g. from the Kaunergrat in the vicinity of the study area (Zangerl, 1997) and the Landeck Quartzphyllite zone further to the north (Headrace Tunnel Prutz-Imst: TIWAG unpublished reports 1953; Landecker Tunnel: Alpen Strassen AG, unpublished reports 1993; Perjen Tunnel: Köhler, 1983). Further, coarse-crystalline carbonate fracture fillings were encountered in biotite-plagioclase-gneiss in the slopes of the Sellrain Valley (Volani, 2012).

Groundwater containing sulphate has also been encountered in the Landeck Quartzphyllite zone especially in the deeply fractured and fragmented rock slopes (e.g. Headrace Tunnel Prutz-Imst, TIWAG, unpublished reports 1953, 1958). Also, calcite was encountered in open fractures in the tunnels. Further, Binet et al. (2009) investigated the groundwater composition at two comparable rockslide-dominated areas in the Southern and Eastern Alps and attributed the local and temporary rise in sulphate concentration to gravitational slope deformations.

The isotopic analyses of the four spring waters in the study area show low $\delta^{34}S$ values in the range of +0.6 to +6.2 ‰ VCDT, very similar to the values (-6 to 0 ‰ VCDT) obtained from groundwater analysed from pyrite-bearing slates in Brixlegg, Tyrol (Millen et al., 2003) and groundwater (-24 to +4 ‰ VCDT) emerging from various sulphide-bearing metamorphic rocks along the Wipp Valley, Tyrol (Lumassegger et al., 2005).

6.4 Conceptual groundwater flow model

Due to the generally low porosity (below 1 %) and low hydraulic conductivities of the bedrock, groundwater flows preferentially within zones of highly weathered bedrock (i.e. the saprolite; cf. Welch and Allen, 2014), brittle fault and fracture zones, deep-seated rockslides, and conductive Quaternary deposits, i.e. alluvial, debris flows, talus and colluvial deposits (Figure 11). Rock glaciers also form localised aquifers in high altitude tributary valleys and cirques and show a high discharge during summer.

The rockslides are generally characterised by rather high hydraulic conductivities (up to about 10^{-4} m/s) and porosities (up to around 26 %) down to depths of more than 100 m. Thus, this high hydraulic conductivity produces a thick vadose zone and reduces the seepage zone within the rockslides, but generally, in the zones of rockslide accumulation at the toe of the slope, springs emerge above areas of lower hydraulic conductivity (Figure 11). This is particularly apparent for two of the rockslides, Hapmes and Nasserein (Figure 1), which are characterised by large total displacements and distinct bulging accumulations at the toe of the slopes.

The main regions of recharge in the study area are the relatively flat tributary valleys and cirques which contain widespread till, talus, and alluvial and colluvial deposits at altitudes above about 2400 m asl. Several springs containing high concentrations of total dissolved solids are situated at the mouth of these tributary valleys emerging at lithological boundaries, e.g. at the contact between more permeable and conductive alluvial or colluvial deposits and less permeable till and/or low conductive bedrock (Figure 11). Given that these tills have a clay- and silt-rich matrix and show a high degree of compaction due to previous loading by ice (especially the basal tills), they often act as aquitards.

Within the fractured bedrock the water most likely circulates along very few, well connected, hydraulically active joints and faults (based on observations in the Klasgarten Exploration Drift and borehole tests; cf. Boutt et al., 2010).

A vadose zone of up to several hundred metres thickness can be assumed below the mountain crests. The results from the comprehensive hydraulic packer tests and permanently installed water gauge measurements in boreholes indicate no upwelling of deep waters.

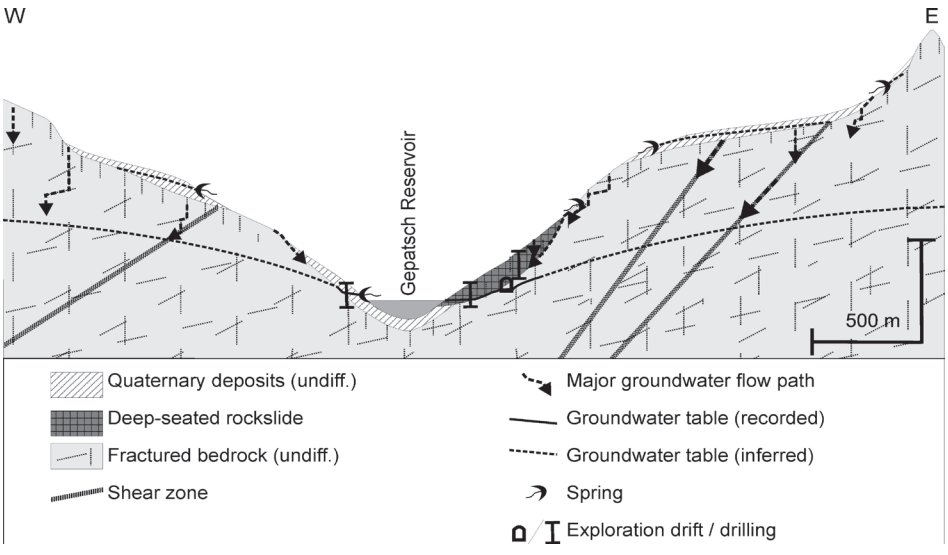

Figure 11: Conceptual groundwater flow model of the study area depicting shallow and deep flow systems.

Some springs are assumed to emerge from a combination of sediment and fractured bedrock aquifers, i.e. perched groundwater flow systems in conductive sediments situated above deep-seated water tables in the fractured bedrock (Figure 11).

7. Conclusions

This study reveals new insights into water-mineral interactions in silicate rock aquifers (i.e. paragneiss and orthogneiss) covered by Quaternary deposits, which can be transferred to comparable settings in other crystalline units of the Alps.

The water is of meteoric origin and is characterised by moderate residence times (<5 years). Both the water from the natural springs and tunnel inflows are dominantly of the Ca-Mg-SO_4 type with EC values of approximately 50-300 µS/cm and approximately 150-300 µS/cm, respectively. The EC values can substantially increase locally to 1400 µS/cm, i.e. the waters can contain high amounts of total dissolved solids.

Further, the hydrochemical analyses indicate that (a) carbonate dissolution and sulphide oxidation play a key role and (b) that gravitational rock disintegration processes causing the development of rockslides etc. increase the hydraulic permeabilities through fragmentation of the rock mass to depths of more than 100 m. Air flow through these fractures and voids drives these reactions. A (Ca+Mg)/SO_4 ratio of 1 is typical of recharge areas affected by rock fragmentation (i.e. mass movements) in the study area. Deep-seated groundwater isolated from the outside atmosphere does not follow this general trend and contains higher amounts of HCO_3 due to limited CO_2 degassing.

Acknowledgements

We thank the TIWAG-Tiroler Wasserkraft AG for providing data from extensive field and laboratory investigations and access to the Klasgarten Exploration Drift and Pitztal and Radurschl Water Conduction Galleries. This study is part of the alpS research projects 'ProMM' and 'AdaptInfra', which are supported by TIWAG, ILF Consulting Engineers, geo.zt and the Austrian Research Promotion Agency (COMET-program). The alpS-K1-Centre is supported by Federal Ministries BMVIT and BMWFW as well as the States of Tyrol and Vorarlberg in the framework of "COMET – Competence Centers for Excellent Technologies". COMET is processed through FFG. The quality of the manuscript was improved by the constructive comments of the co-editor Sylke Hilberg and two anonymous reviewers.

References

Bernhard, F., 2008. Andalusit, Gips, Klinozoisit, Molybdänit, Pyrit, Quarzkristalle, Rutil, ged. Schwefel und Stilbit-Ca aus dem Verpeiltal östlich von Feichten, Kaunertal, Ötztaler Alpen, Tirol. Carinthia II, 198/118, 236-237.

Binet, S., Spadini, L., Bertrand, C., Guglielmi, Y., Mudry, J. and Scavia, C., 2009. Variability of the groundwater sulfate concentration in fractured rock slopes: a tool to identify active unstable areas. Hydrology and Earth System Sciences, 13, 2315-2327. http://dx.doi.org/10.5194/hess-13-2315-2009

Boutt, D.F., Diggins, P. and Mabee, S., 2010. A field study (Massachusetts, USA) of the factors controlling the depth of groundwater flow systems in crystalline fracture-rock terrain. Hydrogeology Journal, 18/8, 1839-1854. http://dx.doi.org/10.1007/s10040-010-0640-y

Bucher, K., Zhu, Y. and Stober, I., 2009. Groundwater in fractured crystalline rocks, the Clara mine, Black Forest (Germany). International Journal for Earth Sciences, 98/7, 1727-1739. http://dx.doi.org/10.1007/s00531-008-0328-x

Bucher, K., Stober, I. and Selig, U., 2012. Water deep inside the mountains: Unique water samples from the Gotthard rail base tunnel, Switzerland. Chemical Geology, 334, 240-253. http://dx.doi.org/10.1016/j.chemgeo.2012.10.031

Clark, I.D. and Fritz, P., 1997. Environmental Isotopes in Hydrogeology. Lewis Publishers, New York, 328 pp.

Craig, H., 1961. Isotopic variations in meteoric waters. Science, 133/3465, 1702-1703. http://dx.doi.org/10.1126/science.133.3465.1702

Cravotta, C.A., K.B.C. Brady, M.W. Smith and Beam, R.L., 1990. Effectiveness of the addition of alkaline materials at surface coal mines in preventing or abating acid mine drainage: Part 1. Geochemical Considerations. In: J. Skousen, J. Sencindiver, D. Samuel, (eds.), Proceedings of the 1990 Mining and Reclamation Conference and Exhibition, 1, pp. 221-225.

Deutsch, W.J., 1997. Groundwater Geochemistry: Fundamentals and Applications to Contamination. Lewis Publishers, New York, 232 pp.

DEV, 1994. Deutsche Einheitsverfahren zur Wasser-, Abwasser- und Schlammuntersuchung, Physikalische, chemische, biologische und bakteriologische Verfahren (German Standard Methods for the Examination of Water, Wastewater and Sludge). Fachgruppe Wasserchemie in der Gesellschaft Deutscher Chemiker in Gemeinschaft mit dem Normenausschuss Wasserwesen (NAW) im DIN Deutsches Institut für Normung e. V. (Ed.), Berlin, 2378 pp.

DIN 38406 E5, 1983. German standard methods for the examination of water, waste water and sludge; cations (group E); determination of ammonia-nitrogen (E 5). German Institute for Standardization, Berlin, 14 pp.

Ehrlich, H.L., 1998. Geomicrobiology: its significance for geology. Earth-Science Reviews, 45/1-2, 45-60. http://dx.doi.org/10.1016/S0012-8252(98)00034-8

EPA 350.1, 1993. Determination of Ammonia Nitrogen by Semi-Automated Colorimetry. Revision 2.0. J.W. Odell (ed.), Environmental Monitoring Systems Laboratory – Office of Research and Development, U.S. Environmental Protection Agency, Cincinnati, Ohio, 14 pp.

Frengstad, B. and Banks, D., 2007. Universal controls on the evolution of groundwater chemistry in crystalline bedrock: the evidence from empirical and theoretical studies. In: J. Krasny and J.M. Sharp (eds.), Groundwater in fractured rocks. Selected papers from the Groundwater in Fractured Rocks International Conference, Prague, 2003. IAH Selected Papers on Hydrogeology, 9, Taylor & Francis Group, London, pp. 275-289. http://dx.doi.org/10.1201/9780203945650.ch18

Götzinger, M.A., Lein, R. and Pak, E., 2001. Geologie, Mine-

ralogie und Schwefelisotopie ostalpiner „Keuper"-Gipse – Vorbericht und Diskussion neuer Daten. Mitteilungen der Österreichischen Mineralogischen Gesellschaft, 146, 95-96.

Hammer, W., 1923a. Erläuterungen zur Geologische Spezialkarte der Republik Österreich, Blatt Nauders (5245). Verlag Geologische Bundesanstalt, Vienna, 62 pp.

Hammer, W., 1923b. Geologische Spezialkarte der Republik Österreich 1:75.000, Blatt Nauders (5245). Verlag Geologische Bundesanstalt, Vienna.

Hölting, B. and Coldewey, W.G., 2013. Hydrogeologie: Einführung in die Allgemeine und Angewandte Hydrologie, 8th Edition. Springer, 438 pp. http://dx.doi.org/10.1007/978-3-8274-2354-2

Holzmann, M. and Hofer, B., 2012. Erkundungen und Verhaltensbeurteilungen einer tiefgründigen Massenbewegung im Kaunertal. Conference Proceedings to the 14th Geoforum Umhausen, 18 October – 19 October 2012, 7 pp.

Kilchmann, S., 2001. Typology of recent groundwaters from different aquifer environments based on geogenic tracer elements. Unpublished PhD thesis, École Polytechnique Féderale de Lausanne, Lausanne, Switzerland, 254 pp. http://dx.doi.org/10.5075/epfl-thesis-2411

Kilchmann, S., Waber, H.N., Parriaux, A. and Bensimon, M., 2004. Natural tracers in recent groundwaters from different Alpine aquifers. Hydrogeology Journal, 12/6, 643-661. http://dx.doi.org/10.1007/s10040-004-0366-9

Köhler, M., 1983. Perjentunnel (Landeck, Tirol): Baugeologische Verhältnisse, Prognose und tektonische Schlussfolgerungen. Geologisch-Paläontologische Mitteilungen Innsbruck, 12, 249-267.

Krainer, K., Mostler, W. and Spötl, C., 2007. Discharge from active rock glaciers, Austrian Alps: A stable istope approach. Austrian Journal of Earth Sciences, 100, 102-112.

Krainer, K. and Ribis, M., 2012. A rock glacier inventory of the Tyrolean Alps (Austria). Austrian Journal of Earth Sciences, 105/2, 32-47.

Kralik, M., Zieritz, I., Grath, J., Vincze, G., Philippitsch, R. and Pavlik H., 2005. Hydrochemische Karte Österreichs – Hydrochemical Map of Austria – Oberflächennaher Grundwasserkörper und Fließgewässer; Mittelwerte von Wassergüteerhebungsdaten (WGEV-Daten) 1991-2001. Umweltbundesamt, Berichte BE-269, 2. Revisted edition, 19 pp.

Kralik, M., 2015. How to estimate mean residence times of groundwater. Procedia Earth and Planetary Science, 13, 301-306. http://dx.doi.org/10.1016/j.proeps.2015.07.070

Krásny, J. and Sharp, J.M. Jr, 2007. Hydrogeology of fractured rocks from particular fractures to regional approaches: State-of-the-art and future challenges. In: J. Krasny and J.M. Sharp (eds.), Groundwater in fractured rocks. Selected papers from the Groundwater in Fractured Rocks International Conference, Prague, 2003. IAH Selected Papers on Hydrogeology, 9, Taylor & Francis Group, London, pp. 1-30.

Lauffer, H., 1968. Das Kaunertalkraftwerk. Österreichische Wasserwirtschaft, 20/7-8, 130-144.

Lauffer, H., Neuhauser, E. and Schober, W., 1967. Uplift responsible for the slope movements during the filling of the Gepatsch reservoir. 9th Int. Congress on large dams- (ICOLD), Istanbul, Turkey, 32/41, 669-693.

Lumassegger, M., Starni, I, Millen, B., Georgi, N. and Mirlach, A., 2005. BBT Hydrogeologische Voruntersuchungen/BBT Indagini preliminari di idrogeologia, Wasserwirtschaftliche Beweissicherung Endbericht 2004/Monitoraggio delle risorse idriche – Rapporto finale 2004 (GEO-D0054). ARGE Hydrogeologie Brenner Basistunnel Starni, ILF, Dierich, unpublished report, 49 pp.

Madritsch, H. and Millen, B., 2007. Hydrogeologic evidence for a continuous basal shear zone within a deep seated gravitational slope deformation (Eastern Alps, Tyrol, Austria). Landslide, 4/2, 149-162. http://dx.doi.org/10.1007/s10346-006-0072-x

Matthess, G., 1994. Die Beschaffenheit des Grundwassers. Lehrbuch der Hydrogeologie 2, 3rd edition, Borntraeger, Berlin, 499 pp.

Matthias, E.P., 1961. Die metallogenetische Stellung der Erzlagerstätten im Bereich Engadin und Arlberg. Berg- und Hüttenmännische Monatshefte, 106, 45-55.

Mazor, E., 2003. Chemical and Isotopic Groundwater Hydrology, 3rd edition. CRC Press, New York, 352 pp.

Merkel, B.J. and Planer-Friedrich, B., 2008. Groundwater Geochemistry – A Practical Guide to Modeling of Natural and Contaminated Aquatic Systems, 2nd edition. Editor: D.K. Nordstrom. Springer, Berlin, 230 pp.

Millen, B., 2003. Aspects of the hydrogeology of a mining region with a focus on the antimony content of the spring-water, Eiblschrofen Massif, Schwaz, Tyrol, Austria. Mitteilungen der Österreichischen Geologischen Gesellschaft, 94, 139-156.

Millen, B. and Brandner, R., 2001. Linking lithofacies to groundwater provenance – examples from the Northern Calcareous Alps, Austria, using the stable sulphur isotope and trace element antimony. 5th Workshop for Alpine Geological Studies, Obergurgl, September 2001, Tyrol, Austria. Geologisch-Paläontologische Mitteilungen Innsbruck, 25, 145.

Millen, B., Brandner, R., Burger, U. and Poscher, G., 2003. The essential geology and hydrogeology for 92km of tunnelling, Austria/Italy. In: J. Krasny and J.M. Sharp (eds.), Groundwater in fractured rocks. Proceedings to the Groundwater in Fractured Rocks International Conference, Prague, 2003, pp. 361-362.

Millen, B. and Spötl, C., 2006. Strukturgeologische Kartierung und ergänzende geologische Studien, Schlussbericht Pos.5.7. „Geochemie und Hydrochemie", Document D0104-G4.1g-01, Rev. 01. Working Group: University of Innsbruck, GBA, CFR for the Brenner Base Tunnel BBT SE (unpublished report), 308 pp.

Mittermayr, F., Bauer, C., Klammer, D., Böttcher, M., Leis, A., Escher, P. and Dietzel, M., 2012. Concrete under sulphate attack: An isotope study on sulphur sources. Isotopes in Environmental and Health Studies, 48/1, 105-117. http://dx.doi.org/10.1080/10256016.2012.641964

Mook, W.G., 2000. Environmental isotopes in the hydrological cycle, IHP-V Technical Documents in Hydrology, No.39

Volumes I-VI, UNESCO/IAEA, Paris/Vienna.

ÖNORM EN ISO 10304-1, 2012. Water quality – Determination of dissolved anions by liquid chromatography of ions – Part 1: Determination of bromide, chloride, fluoride, nitrate, nitrite, phosphate and sulfate (ISO 10304-1:2007 + Cor 1:2010). Austrian Standards Institute, Vienna, 30 pp.

ÖNORM EN ISO 11885, 2009. Water quality – Determination of selected elements by inductively coupled plasma optical emission spectrometry (ICP-OES) (ISO 11885:2007). Austrian Standards Institute, Vienna, 33 pp.

ÖNORM EN 26777, 1993. Water quality – Determination of nitrite – Molecular absorption spectrometric method (ISO 6777:1984). Austrian Standards Institute, Vienna, 7 pp.

ÖNORM EN ISO 5667-3, 2013. Water quality – Sampling – Part 3: Preservation and handling of water samples (ISO 5667-3:2012), 57 pp.

ÖNORM EN ISO 9963-1, 1996. Water quality – Determination of alkalinity – Part 1: Determination of total and composite alkalinity (ISO 9963-1:1994). Austrian Standards Institute, Vienna, 9 pp.

Parkhurst, D.L. and Appelo, C.A.J., 1999. User's guide to PHREEQC (version 2) – A computer program for speciation, batch-reaction, one-dimensional transport, and inverse geochemical calculations. U.S. Geological Survey Water-Resources Investigations Report 99/4259, 312 pp.

Piccolruaz, C., 2004. Zur Quartärgeologie des Kaunergrates im Bereich östlich des Gepatsch-Stausees in den westlichen Ötztaler Alpen (Tirol) unter besonderer Berücksichtigung der Blockgletscher. Unpublished diploma thesis, University of Innsbruck, 135 pp. http://search.obvsg.at/UIB:UIB_aleph_acc001145722

Purtscheller, F., 1978. Sammlung geologischer Führer Nr. 53 – Ötztaler und Stubaier Alpen, 2nd edition. Borntraeger, Berlin, 128pp.

Reichl, P., Probst, G., Erhard-Schippek, W., Goldschmidt, F. and Riepler, F., 2001. Initial hydrogeological and hydrological field investigations for the Koralm Tunnel. Felsbau, 19/6, 37-40.

Rockware Inc., 2006. A User's Guide to Rockware AqQA Version 1.1, Golden, Colorado, USA, 54 pp.

Roether, W., 1967. Estimating the tritium input to groundwater from wine samples: groundwater and direct run-off contribution to central European surface waters. In: IAEA, 1967. Isotope in Hydrology – Proceedings of a Symposium, Vienna, 14-18 November 1966, Vienna, pp. 73-90.

Sacchi, E., Dematteis, A. and Rossetti, P., 2004. Past and present circulation of CO_2-bearing fluids in the crystalline Gran Paradiso Massif (Orco Valley, north-western Italian Alps): tectonic and geochemical constraints. Applied Geochemistry, 19, 395-412. http://dx.doi.org/10.1016/S0883-2927(03)00152-5

Schmid, S.M., Fügenschuh, B., Kissling, E. and Schuster, R., 2004. Tectonic map and overall architecture of the Alpine orogen. Eclogae Geologicae Helvetiae, 97, 93-117. http://dx.doi.org/10.1007/s00015-004-1113-x

Schneider-Muntau, B., 2012. Zur Modellierung von Kriechhängen. Unpublished PhD thesis, University of Innsbruck, 263 pp. http://search.obvsg.at/UIB:UIB_aleph_acc001748715

Schroll, E., 1997. Geochemische und geochronologische Daten und Erläuterungen. In: L., Weber, (ed.), Handbuch der Lagerstätten, Erze, Industrieminerale und Energierohstoffe Österreichs, Archiv für Lagerstättenforschung, 19, pp. 395-538.

Selverstone, J., Axen, G.J. and Bartley, J.M., 1995. Fluid inclusion constraints on the kinematics of footwall uplift beneath the Brenner Line normal fault, eastern Alps. Tectonics, 14/2, 264-278. http://dx.doi.org/10.1029/94TC03085

Singhal, B.B.S. and Gupta, R.P., 2010. Applied Hydrogeology of Fractured Rocks, 2nd edition, Springer, New York, 408 pp.

Sonnleitner, R., Redl, B. and Schinner, F., 2011. Microbial mobilization of major and trace elements from catchment rock samples of a high mountain lake in the European Alps. Arctic, Antarctic and Alpine Research, 43/3, 465-473. http://dx.doi.org/10.1657/1938-4246-43.3.465

Spötl, C., 1988a. Zur Altersstellung permoskythischer Gipse im Raum des östlichen Karwendelgebirges (Tirol). Geologisch-Paläontologische Mitteilungen Innsbruck, 14, 197-212.

Spötl, C., 1988b. Evaporitische Fazies der Reichenhaller Formation (Skyth/Anis) im Haller Salzberg (Nördliche Kalkalpen, Tirol). Jahrbuch Geologische Bundesanstalt, 131/1, 153-168.

Spötl, C., 1988c. Sedimentologisch-fazielle Analyse tektonisierter Evaporitserien – eine Fallstudie am Beispiel des Alpinen Haselgebirges (Permoskyth, Nördliche Kalkalpen). Geologisch-Paläontologische Mitteilungen Innsbruck, 15, 59-69.

Spötl, C. and Pak, E., 1996. A strontium and sulfur isotopic study of Permo-Triassic evaporites in the Northern Calcareous Alps, Austria. Chemical Geology, 131/1, 219-234. http://dx.doi.org/10.1016/0009-2541(96)00017-4

Spötl, C., Unterwurzacher, M., Mangini, A. and Longstaffe, F.J., 2002. Carbonate speleothems in the dry, inneralpine Vintschau valley, northernmost Italy: witnesses of changes in climate and hydrology since the last glacial maximum. Journal of Sedimentary Research, 72/6, 793-808. http://dx.doi.org/10.1306/041102720793

Stichler, W. and Herrmann, A., 1983. Application of environmental isotope techniques in water balance studies of small basins. In: Van der Beken, A. and Herrmann, A. (eds.), New Approaches in Water Balance Computations, IAHS, Hamburg Symposium, August 1983, IAHS-148: 93-112.

Strauhal, T., 2009. Mineralogische und geotechnische Eigenschaften von tektonisch- und massenbewegungsbedingten Kakiriten. Unpublished diploma thesis, University of Innsbruck, 245 pp. http://search.obvsg.at/UIB:UIB_aleph_acc001593853

Tentschert, E., 1998. Das Langzeitverhalten der Sackungshänge im Speicher Gepatsch (Tirol, Österreich). Felsbau, 16/3, 194-200.

Thies, H., Nickus, U., Tolotti, M., Tessadri, R. and Krainer, K., 2013. Evidence of rock glacier melt impacts on water chemistry and diatoms in high mountain streams. Cold Regions Science and Technology, 96, 77-85. http://dx.doi.org/10.1016/j.coldregions.2013.06.006

Tóth, J., 1999. Groundwater as a geologic agent: An overview of the causes, processes, and manifestations. Hydrogeology Journal, 7/1, 1-14. http://dx.doi.org/10.1007/s100400050176

van Husen, D., 1987. Die Ostalpen und ihr Vorland in der letzten Eiszeit (Würm), 1:500.000. Die Ostalpen in den Eiszeiten (Würm), Geologische Bundesanstalt, Vienna, 24 pp.

Vavtar, F., 1979. Syngenetische metamorphe Kiesanreicherungen in Paragneisen des Ötztal-Kristallins (Kaunertal, Tirol). Veröffentlichungen Museum Ferdinandeum, 59, 151-163.

Vavtar, F., 1988. Die Erzanreicherungen im Nordtiroler Stubai-, Ötztal- und Silvrettakristallin. Archiv für Lagerstättenforschung, 9, 103-153.

Vavtar, F., 1997. Polymetallischer Cu-Fe-Zn-Pb-Erzbezirk Stubai-Ötztal. In: L., Weber, (ed.), Handbuch der Lagerstätten, Erze, Industrieminerale und Energierohstoffe Österreichs, Archiv für Lagerstättenforschung 19, pp. 297-299.

Volani, M., 2012. Strukturell induzierte Massenbewegung am Freihut bei Gries im Sellrain (Sellraintal, Tirol). Unpublished diploma thesis, University of Innsbruck, 103 pp. http://search.obvsg.at/UIB:UIB_aleph_acc001789848

Weber, L. (ed.), 1997. Handbuch der Lagerstätten, Erze, Industrieminerale und Energierohstoffe Österreichs, Archiv für Lagerstättenforschung 19, Geologische Bundesanstalt, Vienna, 607 pp.

Welch, L.A. and Allen, D.M., 2014. Hydraulic conductivity characteristics in mountains and implications for conceptualizing bedrock groundwater flow. Hydrogeology Journal, 22/5, 1003-1026. http://dx.doi.org/10.1007/s10040-014-1121-5

White, A.F., Bullen, T.D., Vivit, D.V., Schulz, M.S. and Clow, D.W., 1999. The role of disseminated calcite in the chemical weathering of granitoid rocks. Geochimica et Cosmochimica Acta, 63/13-14, 1939-1953. http://dx.doi.org/10.1016/S0016-7037(99)00082-4

White, A.F., Schulz, M.S., Lowenstern, J.B., Vivit, D.V. and Bullen, T.D., 2005. The ubiquitous nature of accessory calcite in granitoid rocks: Implications for weathering, solute evolution, and petrogenesis. Geochimica et Cosmochimica Acta, 69/6, 1455-1471. http://dx.doi.org/10.1016/j.gca.2004.09.012

Zangerl, C., 1997. Kristallingeologische und petrologische Untersuchungen im vorderen Pitz- und Kaunertal. Unpublished diploma thesis, University of Innsbruck, 101 pp. http://search.obvsg.at/UIB:UIB_aleph_acc000355000

Zangerl, C., Eberhardt, E. and Perzlmaier, S., 2010. Kinematic behaviour and velocity characteristics of a complex deep-seated crystalline rockslide system in relation to its interaction with a dam reservoir. Engineering Geology, 112/1-4, 53-67. http://dx.doi.org/10.1016/j.enggeo.2010.01.001

Zangerl, C., Engl, D., Prager, C. and Strauhal, T., 2013. Tiefgründige Massenbewegungen im Einflussbereich des Speichers Gepatsch (Kaunertal) – alpS Forschungsbericht Teil A, Rev. 1, alpS – Internal Report, Innsbruck, 168 pp.

Received: 19 May 2015
Accepted: 30 October 2015

Thomas STRAUHAL[1) 2)*)], Christoph PRAGER[1) 3)], Bernard MILLEN[4)], Christoph SPÖTL[2)], Christian ZANGERL[1) 5)] & Rainer BRANDNER[2)]

[1)] alpS – Centre for Climate Change Adaptation, Grabenweg 68, 6020 Innsbruck, Austria;

[2)] Institute of Geology, University of Innsbruck, Innrain 52f, 6020 Innsbruck, Austria;

[3)] ILF Consulting Engineers Austria GmbH, Feldkreuzstraße 3, 6063 Rum, Austria;

[4)] GEOCONSULT Consulting Engineers, Hölzlstraße 5, 5071 Wals, Austria;

[5)] Institute of Applied Geology, University of Natural Resources and Life Sciences, Peter-Jordan-Straße 70, 1190 Vienna, Austria;

[*)] Corresponding author, strauhal@alps-gmbh.com